DOKUZ EYLÜL UNIVERSITY

GRADUATE SCHOOL OF NATURAL AND APPLIED SCIENCES

# MONITORING AND EXPLORING NATURAL HAZARD RISK IN TEOS ANCIENT CITY USING REMOTE SENSING AND GIS

by

Fatih YILDIZ

October, 2022

İZMİR

# MONITORING AND EXPLORING NATURAL HAZARD RISK IN TEOS ANCIENT CITY USING REMOTE SENSING AND GIS

**A Thesis Submitted to the**

**Graduate School of Natural and Applied Sciences of Dokuz Eylül University**

**In Partial Fulfillment of the Requirements for the degree of Master of Science in Geographical Information Systems Program**


**by**

**Fatih YILDIZ**


**October, 2022**

**İZMİR**

**M.Sc THESIS EXAMINATION RESULT FORM**

We have read the thesis entitled "**MONITORING AND EXPLORING NATURAL HAZARD RISK IN TEOS ANCIENT CITY USING REMOTE SENSING AND GIS**" completed by **FATİH YILDIZ** under supervision of **ASST. PROF. DR. A. HÜSNÜ ERONAT** and we certify that in our opinion it is fully adequate, in scope and in quality, as a thesis for the degree of Master of Science.

……………………………………………..

Asst. Prof. Dr. A. Hüsnü ERONAT

Supervisor

| | |
|---|---|
| ………………………………….. | ……………………………….. |
| Assoc. Prof. Dr. Ali GÜL | Prof. Dr. M. Kirami ÖLGEN |
| (Jury Member) | (Jury Member) |

Prof. Dr. Okan FISTIKOĞLU

Director

Graduate School of Natural and Applied Sciences

## ACKNOWLEDGMENT

I would like to express my special thanks of gratitude to my thesis advisor Asst. Prof. A. Hüsnü Eronat for not only being my thesis advisor and guiding me every step of the way, but also for showing me the power of education and demonstrating how kind and loving teachers can be.

I also would like to thank Assoc. Prof. Fethi Bengil and Sue Eronat for their unconditional support. I would like to thank my parents and brother for everything. I am grateful to the Department of Scientific Research Projects at Dokuz Eylül University for including my thesis in the scope of Scientific Research and for all their support (Scientific Research Project Number: 2021.KB.FEN033). I would also like to thank General Directorate of Mapping for providing me orthophoto images that include the study area and also would like to thank İTÜ UHUZAM for high resolution satellite images. Lastly, I want to thank Prof. Dr. Musa Kadıoğlu from Ankara University for his support and convenience for me to be able to work in Teos Ancient City.

Fatih YILDIZ

**MONITORING AND EXPLORING NATURAL HAZARD RISK IN TEOS ANCIENT CITY USING REMOTE SENSING AND GIS**


## ABSTRACT

Both natural and human-induced risks have posed a threat to residential areas and important artifacts from past to present. Since cultural heritages are structures coming from the past, they are more vulnerable to several threats. This research work was conducted to define natural and anthropogenic hazard risk factors which possibly can affect the integrity and the permanence of Teos Ancient City and to find solutions for these risk factors. High resolution satellite images taken in different years were utilized in order to effectively carry out the research work based on revealing the changes in urban sprawl and transportation route lengths from past to present in Teos. Soil erosion risk and coastal flood risk analyzes were conducted with the created Digital Elevation Model. Unmanned Aerial Vehicle (UAV) flights were carried out to observe the most up-to-date status of the ruins in Teos. Analytic Hierarchy Process (AHP) method was used to identify the risk factors of highest importance. After the realization of the AHP analysis, The most important among the risk factors for Teos were determined as urban sprawl, proximity to transportation routes and earthquake. In conclusion, some important risks in Teos were determined, thus it was observed that regulations and control mechanisms have to be reviewed more frequently.



**Keywords:** Cultural heritage, natural hazards, GIS, remote sensing, natural and anthropogenic risks, Analytic Hierarchy Process

**TEOS ANTİK KENTİ'NDE DOĞAL TEHLİKE RİSKİNİN UZAKTAN ALGILAMA VE CBS KULLANILARAK İZLENMESİ VE ARAŞTIRILMASI**

# ÖZ

Gerek doğal gerekse insan kaynaklı riskler geçmişten günümüze kadar yerleşim alanları ve önemli eserler için tehdit oluşturmuştur. Kültürel miraslar geçmişten kalan yapılar oldukları için çeşitli tehditlere karşı daha savunmasızdırlar. Bu araştırma, Teos Antik Kenti'nin bütünlüğünü ve kalıcılığını etkileyebilecek doğal ve insan kaynaklı tehlike içeren risk faktörlerini tanımlamak ve bu risk faktörlerine çözüm bulmak amacıyla yapılmıştır. Teos'ta geçmişten günümüze kentsel yayılma ve ulaşım yollarının uzunluklarındaki değişimin ortaya konulmasına dayalı araştırma çalışmasının etkin bir şekilde yürütülebilmesi için farklı yıllarda çekilmiş yüksek çözünürlüklü uydu görüntülerinden yararlanılmıştır. Oluşturulan Sayısal Yükseklik Modeli ile toprak erozyonu riski ve kıyı taşkın risk analizleri yapılmıştır. Teos'taki kalıntıların en güncel durumunu gözlemlemek için İnsansız Hava Aracı (İHA) uçuşları gerçekleştirilmiştir. Analitik Hiyerarşi Prosesi (AHP) yöntemi, en yüksek öneme sahip risk faktörlerini belirlemek için kullanılmıştır. AHP analizi sonucunda Teos için en önemli üç risk faktörü kentsel yayılma, ulaşım yollarına yakınlık ve deprem olarak belirlenmiştir. Sonuç olarak Teos'ta bazı önemli riskler tespit edilmiş, bu nedenle düzenlemelerin ve kontrol mekanizmalarının daha sık kurulması gerektiği görülmüştür.

**Anahtar kelimeler:** Kültürel miras, doğal tehlikeler, CBS, uzaktan algılama, doğa ve insan kaynaklı riskler, Analitik Hiyerarşi Proses

**CONTENTS**

## LIST OF FIGURES

**Page**

## LIST OF TABLES

**Page**

**ABBREVIATIONS**

| | |
|---|---|
| GIS | : Geographical Information Systems |
| UAV | : Unmanned Aerial Vehicle |
| AHP | : Analytic Hierarchy Process |
| BC | : before Christ |
| n.d. | : no date |
| TÜİK | : Türkiye İstatistik Kurumu |
| Mw | : Moment magnitude |
| km | : kilometer |
| InSAR | : Interferometric Synthetic Aperture Radar |
| SAR | : Synthetic Aperture Radar |
| LiDAR | : Light Imaging Detection and Ranging |
| TLS | : Terrestrial Laser Scanning |
| UAV-RS | : Unmanned Aerial Vehicles with Remote Sensing |
| DInSAR | : Differential Synthetic Aperture Radar Interferometry |
| PSI | : Persistent Scatterer Interferometry |
| AHP-OS | : AHP online system |
| CORINE | : Coordination of Information on the Environment |
| Fig. | : Figure |
| DEM | : Digital Elevation Model |
| $km^2$ | : square kilometer |

# CHAPTER 1
# INTRODUCTION

Cultural heritages are the immutable traces left by societies to future generations. Each cultural heritage contains social, economic and cultural elements of the period in which it takes place. Language, belief and folk traditions of societies are abstract aspects and all these form a part of culture. Among the factors that make up cultures, there are customs, religious understandings and behavior patterns specific to societies that provide the intersection of traditions and religious understandings. Cultural values that express the belonging of societies should be protected.

Cultural heritages, which are in danger of extinction due to the necessity of preserving the historical values they contain and being built in the past, are faced with human-based risk factors (Ilies et al., 2020, p. 1103), as well as nature-based risks (Ilies et al., 2020, p. 1103).

Human and natural elements that threaten cultural assets can cause serious damage and even permanent extinction (Ilies et al., 2020, p. 1103).

Cultural heritage are in danger of security due to the structure of nature and the reasons this natural structure brings with it (Frodella et al., 2020 as cited in Ilies et al., 2020, p. 1104). It is a serious need to protect the living cultural heritage that have survived from the past to the present. Meeting this need is possible by detailed analysis of risk factors and reducing the possible negative consequences of risks as a result of these analyses (Vojtekova & Vojtek, 2020 as cited in Ilies et al., 2020, p. 1104).

With the development of technology, alternative solutions have emerged for the risk analysis and protection of cultural heritage (Ilies et al., 2020, p. 1104). These techniques are GIS and digitization approaches, which have the advantages of being coherent, user-friendly and affordable. Current researches use GIS methods to observe the details of cultural heritage in an organized and unified way (Ilies et al., 2020, p. 1104).

Digitization aims to create geometric models that aim high accuracy in the long term, examine future transformation and restructuring in the matter of any calamity (Ilies et al., 2020, p. 1104).

The validity of this concept has been confirmed by many researches on the evaluation and protection of cultural heritage (Ilies et al., 2020, p. 1104).

Up-to-date technologies with remote sensing since the time they were developed have played an important role in the preservation of cultural assets (Agapiou et al., 2015, p. 230).

Within the systems containing remote sensing, analyzes that help decision-making are carried out effectively in order to examine the changes caused by environmental effects, to detect possible harmful situations and to prevent such situations before they occur (Agapiou et al., 2015, p. 230).

Since remote application methods are integrated with Geographic Information Systems, cultural assets can be observed effectively, without delay and goal-oriented (Agapiou et al., 2015, p. 230).

In large study areas where in-situ observations will take a lot of time, much faster and relatively affordable results can be obtained when satellite images are used (Agapiou et al., 2015, p. 230).

Cultural elements of a society and traditions from the past are represented by cultural heritages (Nicu, 2017a as cited in Ilies et al., 2020, p. 1103). This bond that enables cultural heritages to come from the past to the present (Indrie et al., 2019 as cited in Ilies et al., 2020, p. 1103) has a great importance in terms of forming a sense of belonging to societies and cultural authenticity (Ilies et al., 2020, p. 1103).

Capabilities to interact with memory (Vecco, 2010 as cited in Ilies et al., 2020, p. 1103) has the greatest share in the permanence of cultural heritage. Society chooses to protect works of such great value (Ilies et al., 2020, p. 1103).

Conservation is more than just preserving the appearance of physical ruins. The ambience, character, and the living pieces of history are preserved by conserving cultural heritages. Cultural heritage should be protected not only because they are historical buildings but also because they represent the unchanging identity of societies. Additionally, architectural elements from the past contribute to the development of beauty of streetscapes.

By keeping the cultural assets alive and transferring them to future generations, all segments of the society will have preserved their identities and left a unique legacy to the next generations.

Aim of this study is to define natural and anthropogenic hazard risk factors which possibly can affect the integrity and the permanence of Teos Ancient City and to find solutions for these risk factors. The fact that to present no study has been conducted related to conserving Teos Ancient City against natural and anthropogenic risks and natural hazards that have affected Sığacık town recently created an awareness and become the motivation for this study.

There is a need for natural protection in this study area, where archaeological studies are quite intense. Coastal areas, which are also part of the study area, are ecologically important. Sustainable coastal management is required not only to safeguard Teos Ancient City's Southern Port, but also to combine the social, cultural, ecological, and economically productive components of the coastal environs.

## 1.1 Study Area

### *1.1.1 Location of Teos*

Located on the coast of Ionia, Teos was a historical Greek city built on a peninsula between Chytrium and Myonnesus. Although the date of its foundation is not clear, it was founded by Minyans from Orchomenus, Ionians and Boeotians. The Ionian League consisted of 12 cities, and Teos was one of them. Teos was located on a low hill. The remaining parts of the ancient city are located in the southern part of a coastal town called Sığacık, which is connected to the district of Seferihisar in İzmir. ("Teos," 2022) (Fig 1.1).

Town of Sığacık can be located at 38°11′N 26°47′E. Distance from Sığacık to the center of Seferihisar can be observed as 5 kilometres (3.1 mi). It is located on a peninsula oriented to the north ("Sığacık," 2022).

Teos, located in the Sığacık district of Seferihisar in the southwest of İzmir, consists of the Acropolis, the ancient harbor and the Hellenistic city walls in general terms (Kadıoğlu, 2012, p. 2).

The borders of Teos Ancient City are marked with a red outline and its position relative to Seferihisar and Sığacık appears in Figure 1.1


Figure 1.1 Location of Teos Ancient City (Red Outline) (Source: ©Google Maps, 2021)

After the excavation process realized between 2010 and 2015, detailed borders of Teos Ancient City were discovered and they can be seen in Figure 1.2.


Figure 1.2 Detailed borders of Teos Ancient City (Polat, 2016)

### *1.1.2 Archaeological Research Background in Teos*

Kadıoğlu (2018, pp. 3-4) explained that since the beginning of the 18th century, Teos has attracted the attention of researchers in the West. The first excavations and simultaneous researches in the city were carried out in 1764-1765. Turkish scientists started their excavations and researches in Teos in the 1960s. Chronologically, Yusuf Boysal and Baki Öğün from Ankara University directed the excavations in 1962-1967; then, between 1980-1992, architect Duran Mustafa Uz directed a small number of excavations. This was followed by the studies of Numan Tuna from Middle East Technical University between 1993-1996. Finally, Prof. Dr. Musa Kadıoğlu from Ankara University (Faculty of Letters, Department of Classical Archeology) has been carrying out excavation, research and conservation works in Teos since 2010.

### *1.1.3 History of the City*

According to Kadıoğlu (2018, p.5), researches have revealed that the Teos region has been used as a settlement since the Protogeometric Period. Thales suggested that Teos was supposed to be the center of Ionia because of its useful placement. Increasing commercial relations in the beginning of 600 BC and so on reached as far as Egypt but due to the conquest of Teos by the Persian commander Harpagos in 545 BC and the increasing Persian pressure, the people of Teos had to leave where they had been settled and established Abdera (around Xanthi) in Thrace (Figure 1.3). Some of those who had to leave Teos and went to Abdera returned to Teos later. Also, approximately in 544 BC, the people living in Teos built the city of Phanagoria in the location of the Taman Peninsula, but soon returned to their homeland of Ionia. (Figure 1.3). Teos, which held a great wealth, gave serious support with seventeen ships in the Battle of Lade.


Figure 1.3 Colonies of Teos in the 6th Century BC (Kadıoğlu, 2018)

Teos, which has its name written on the pages of history culturally, has hosted names such as Antimachus and Anacreon who were well-known poets, the philosophers Nausiphanes and Democritus, the historian Hecataios and the famous book collector Apellicon (Kadıoğlu, 2018, pp. 5-6).

### *1.1.4 Urban Development and the Buildings*

Kadıoğlu (2018, p.7) defined that observations revealed that the orthogonal street structure was not located in Teos. The results that indicate the fact that the streets are neither in perpendicular nor parallel form respectively have showed that the city was not demolished severely during the Persian invasion. The property structure and infrastructure in Teos from 1000 BC were maintained until the traces of the Roman Empire were erased from history.

#### *1.1.4.1 Acropolis*

According to Kadıoğlu (2018, pp. 7-8), Teos Acropolis is on a hill called Kocakır Hill, which can be observed from the location where both of the northern and southern ports stand. The roots of the Acropolis, represented in the Roman Period, go back to the Archaic Period, according to W. Hoepfner. Observation results dating back to 630-590 BC show that the building hosted religious rituals.

#### *1.1.4.2 Temple of Dionysus*

Kadıoğlu (2018, pp. 9-10) explains that temple is seen as one of the most valuable structures of the ancient city which is located within the Hellenistic walls. Some blocks and friezes found in the temple are thought to date back to the Hellenistic period.

#### *1.1.4.3 Theatre*

According to Kadıoğlu (2018, p.11), although Theatre, located on the southeast slopes of the Acropolis, was built according to Greek traditions, no pre-Roman findings have been observed until today.

#### *1.1.4.4 Bouleuterion (Senate House)*

Bouleuterion stands out as the best preserved ruin in Teos. According to Polythros, proficiency tests by grammar and music teachers had been moved to the Bouleuterion. Accordingly, it can be concluded that the Bouleuterion hosted other purposes besides political meetings (Kadıoğlu, 2018, pp. 13-14).

#### *1.1.4.5 Hellenistic City Wall*

Kadıoğlu (2018, p.17) explains the walls are well preserved, from the Acropolis to the South Harbor, and this area is the best studied part of the walls as a result of excavations.

#### *1.1.4.6 South Harbour (Southern Port)*

According to Kadıoğlu (2018, p.19), Teos, one of the most important cities of Ionia, had ports in both the north and south. Although there is no significant remains of the port in the north, the South Port has been well preserved and has survived to the present day.

# CHAPTER 2
# RESEARCH REVIEW

*Natural hazards such as floods, storms, landslide, and tropical cyclones have caused environmental damages and loss of human lives. Flood hazard is one of the most frequent phenomena in the world. As summarized by Sivakumar (2005, p.4), during 10 years (1993–2002) there were 2,654 hazard events in the world where floods and windstorms accounted for approximately 70% of the hazards while the remaining 30% of the disasters were brought about by droughts, landslides, forest fires, heat waves and others (Marfai et al., 2008, p.1507)* (Fig. 2.1).

According to Centre for Research on the Epidemiology of Disasters United Nations Office for Disaster Risk Reduction & Wallemacq, House, (2018), between 1998 and 2017, 1.3 million people died and 4.4 billion were injured, lost their homes, or were displaced as a result of climate-based and geophysical disasters. Earthquakes and tsunamis are among the most damaging phenomena. In addition, drought, storm and flood are natural events that should be considered.

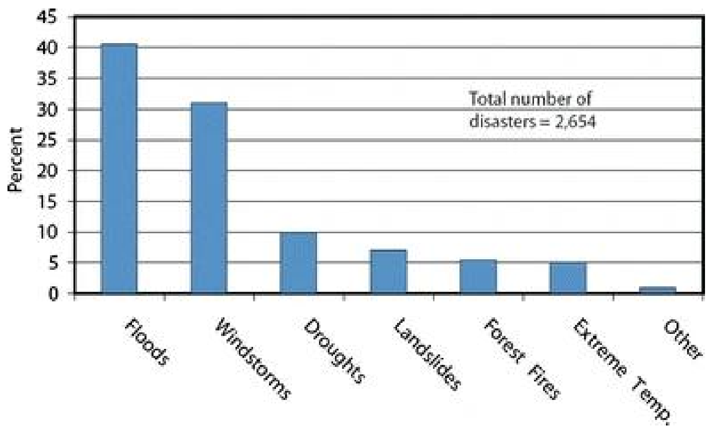


Figure 2.1 Natural hazard events (Sivakumar, 2005, p.5)

## 2.1 Risk Factors

Risk analyzes are important both to reveal the sociological situation and to make the natural environment sustainable. Due to the lack of studies conducted on the risk factors that may threaten Teos at present, the following factors will be analyzed

(Figure 2.2).

For each risk analysis, the appropriate material and method that will allow risk analysis to be performed will be used. As a result of all risk analyzes, it is aimed to reveal the risk factors that threaten the ancient city of Teos the most.

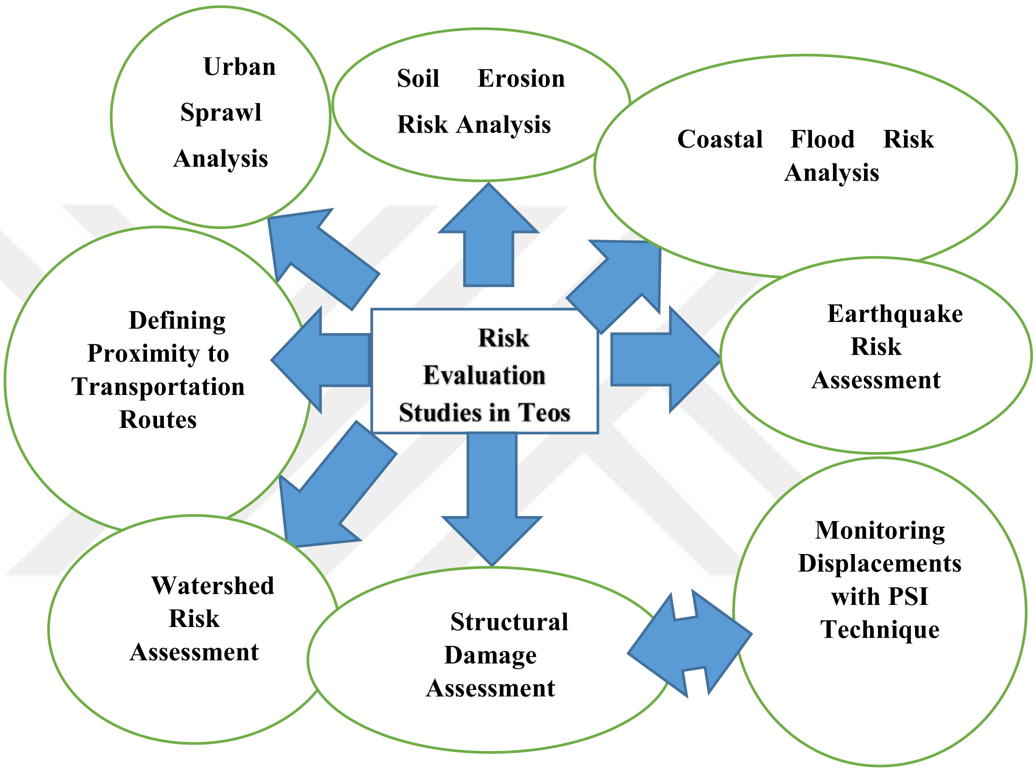


Figure 2.2 Risk evaluation studies in Teos Ancient City

### *2.1.1 Urban Sprawl Analysis*

Deelstra & Girardet (2000) stated that urban development leads to land structure, land use and, accordingly, ecosystem change caused by humans.

Urban sprawl is a factor that negatively affects the ecosystem and prevents the efficient use of the environment both in rural and urban terms (Congedo and Macchi, 2015).

As stated in Urban Sprawl (2021), urban sprawl is a concept that forces people to travel long distances between trade centers, workplaces and homes in a poorly planned city without considering all factors, and also negatively affects nature and other living things.

Some of the effects of urban sprawl can be counted as increasing level of pollution in air and water, higher water consumption due to population, deteriorated human health, decrease in green areas, farmlands and fauna, increasing traffic congestion and flood risk rate (Urban Sprawl, 2021).

Izmir, which has a population of about 4 million, is Turkey's third-largest city (Yakut et al., 2021). According to the data published by Türkiye İstatistik Kurumu (TÜİK) in 2021, annual population growth rate of Izmir province between 2019 and 2020 was 6.3% while the annual population growth rate of Seferihisar district was 8.52% .

As seen on population change graph (Fig. 2.3) and on total population change graph (Fig. 2.4) made with the data provided from TÜİK (2021), in 1965, total population of Seferihisar district was 9,661, the urban population was 5,269 while the rural population was 4,392; until 2007, urban and rural population were almost equal, as of 2007, urban population became 1.5 times more than the rural population; in 2007, urban population was 16,114 while the rural population was 9,716. In 2008, rural population demonstrably decreased to 3,276 while the urban population showed an increase to 23,669. Since 2013, there is no sufficient rural population data that the total population is equal to the urban population. As of 2020, total population of Seferihisar district is 48,320. As for the town of the study area: Sığacık, the actual total population is 3,637 while 32% is elderly (65 years and older) and 18% is young population (TÜİK, 2021).

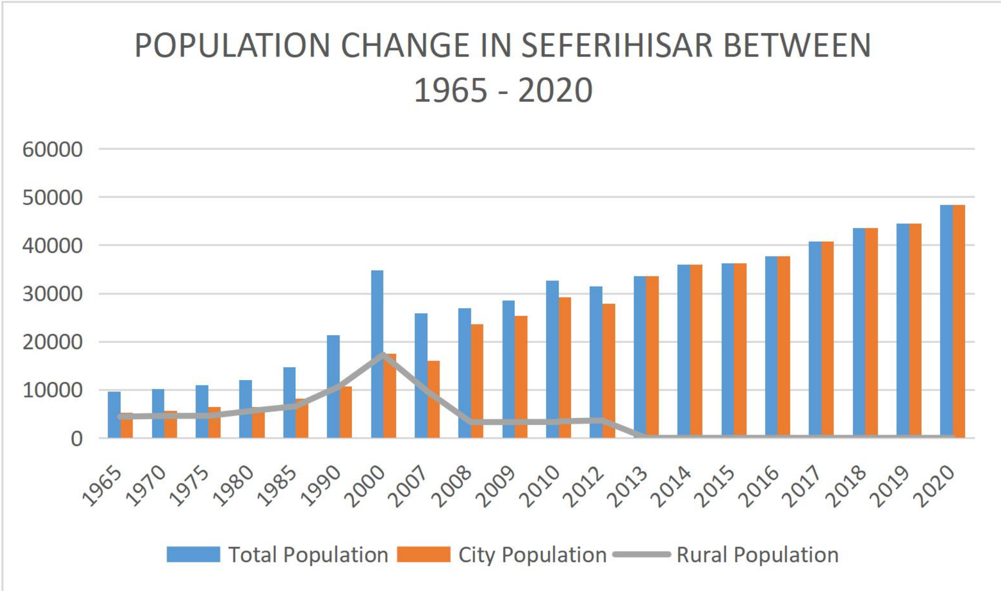


Figure 2.3 Total Population Change in Seferihisar Between 1965-2020 (Graph made by using the data obtained from (TÜİK, 2021)

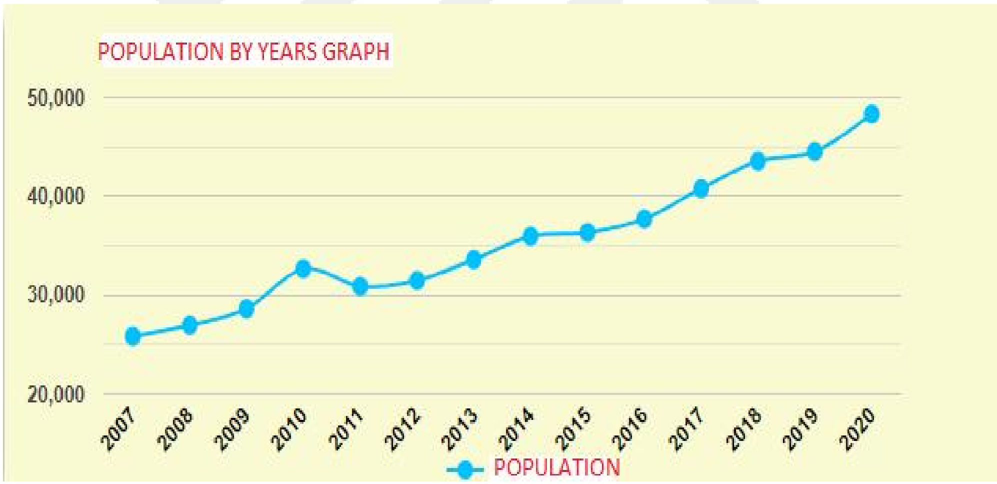


Figure 2.4 Total population change in Seferihisar between 2007 – 2020 (Graph made by using the data obtained from (TÜİK, 2021)

Supervised Classification analysis will be used for urban sprawl detection in the study area. In order to process satellite images, an empirical classification algorithm known as *Maximum Likelihood* classifier will be utilized.

#### *2.1.1.1 Supervised Classification*

Killeen et al. (2015, p.492) stated that supervised classification analysis provides the display and representation of areal data of each unit to be classified. Maximum likelihood is one of the most frequently used algorithms today, which uses statistics, functions and data suitable for the fields to be classified.

Foody (2002) emphasizes the importance of accuracy evaluation during remote sensing based land-cover mapping process to be able to assess the end product in remote sensing thus the quality improvement of the classification can be ensured.

### ***2.1.2 Defining Proximity to Transportation***

United States Environmental Protection Agency (2014) stated that pollution emitted into the air from all kinds of motor vehicles is more common on roads with high density due to the passing of more vehicles. Nitrogen dioxide (NO2) and ozone (O3) were observed in the atmosphere, especially around the roads with high traffic density.

Varotsos et al. (2009, p.590) explained that polluted substances in the atmosphere play a negative role in the deterioration of the condition of both buildings and cultural heritage. When these pollutants are combined with environmental effects, the damage they cause increases exponentially.

The amounts of these gases in the study area were not measured, but it was concluded that negative effects would occur as a result of the increase in vehicle traffic due to the increase in roads

The negative effects of air pollution are not only seen on buildings, but also on people. According to (DeJarnett et al., 2015, p.2), “close proximity to roadways has been associated with the health problems of increased coronary artery disease mortality, myocardial infarction, heart failure, deep vein thrombosis and stroke mortality.”

The proximity of houses to public transport networks is a key factor in explaining urbanization. The increase in the road networks over the years near the ancient city of Teos, which is the study area, will be examined by digitizing orthophoto images.

### *2.1.3 Soil Erosion Risk Analysis*

Siswanto & Sule (2019, p.1) stated that the steep slope is seen as one of the important triggers of erosion. Although there are other factors that affect soil erosion, slope has a significant importance in defining soil erosion. The steep slope will increase the amount and velocity of runoff, thereby accelerating erosion due to more transported and dissolved material. Generally, places with slopes of 8-15%, 15-25%, 25-40% have erosion risk.

Within the scope of this study, a slope map was created to determine soil erosion risk in Teos Ancient City.

### *2.1.4 Watershed Risk Assessment*

USGS (2019) stated that water covers about 71% of the Earth's surface. In this case, the land covering the earth would be approximately 29%. According to Hooke et al. (2013), more than half of the natural land cover is estimated to have been altered by human action, as a result, situations that influence natural water resources and their quality emerged.

Urbanization and the resulting deforestation and desertification are among the factors that negatively affect water resources.

In Fig. 2.5, climate graph and rain measures of Seferihisar in a year can be observed on (Climate-data.org, 2022).

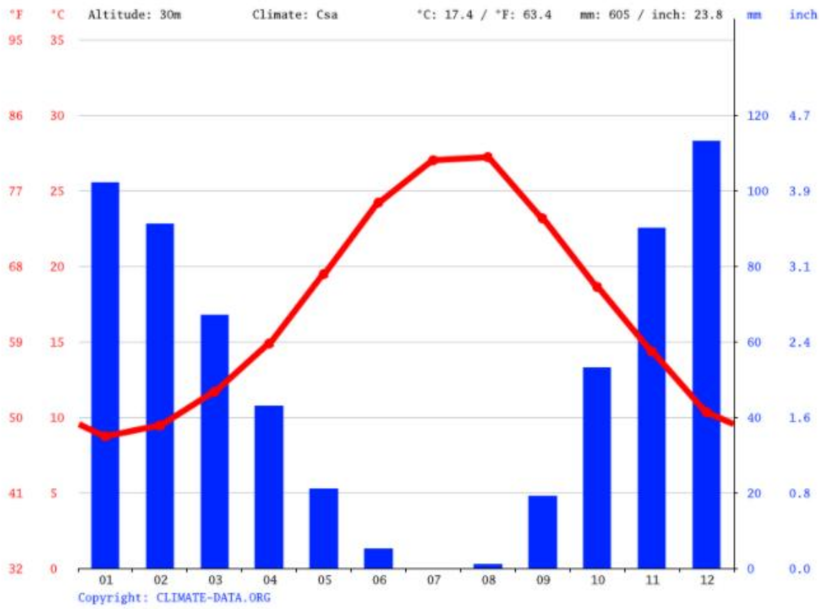


Figure 2.5 Climate graph of Seferihisar (Climate-data.org, 2022)

According to the definition of Sesli Sözlük (2022), “a watershed is a land area within which water flows down to a specific body of water, such as a river, lake, or a drainage basin.”

Topographic boundaries between two or more neighbouring catchment basins, such as a ridge or a crest, also form a watershed. The health of local streams is severely impacted by urbanization.

United States Environmental Protection Agency (2022) explained the watershed as a hydrologically-bounded ecosystem and that watershed management helps to identify the problems associated with ground and surface waters, to observe the effects of these problems on the environment and people, and to find solutions.

Major drainage networks will be identified and a watershed inventory will be developed for environmental risk assessment in Teos Ancient City. The created Digital Elevation Model (DEM) will be used to delineate the watersheds in the study area.

### *2.1.5 Coastal Flood Risk Analysis*

Samanta et al. (2014, p. 961) explained that factors causing coastal flooding include storm surges and/or extreme high tidal waves flooding low coastal areas.

In densely populated coastal urban areas, rapid urbanization has significantly increased susceptibilities. Sığacık is a coastal town whose population and the urban sprawl have recently escalated, therefore it is crucial to monitor coastal flood risks to avoid possible hazards.

"The earthquake that occurred on October 30, 2020, (Mw=6.9) triggered a tsunami that resulted in the death of one person. This person was the first to die because of a tsunami in Turkey" (Onat et al., 2022, p.78).

Özacar et al. (2020, p.17) observed the maximum tsunami height measured as 2.31 m. The maximum wave run-up, which can be explained as the distance between the mean sea level and the highest point of wave crest that touches the structure (Diwedar, 2016), was calculated as 3.82 m in Akarca Region.

According to the studies of Özacar et al. (2020, p.16) carried out in the field and the statements of the people who were in the region at the time of the incident, it was concluded that the places that were most heavily affected after the earthquake were Sığacık Marina, Sığacık Bay and Akarca region. The distance of these places to the epicenter was seen as 30 km. Tsunami generation zone, distribution of the tsunami wave and wave run-up were seen spatio-temporally in the study of Özacar et al. (2020, p.16) (Fig. 2.6, Fig. 2.7 & Fig. 2.8).

Figure 2.6 Before the beginning of tsunami (Özacar et al., 2020, p.16)

Figure 2.7 14 seconds after the beginning of tsunami (Özacar et al., 2020, p.16)

Figure 2.8 34 seconds after the beginning of tsunami (Özacar et al., 2020, p.16)

For hypothetical scenarios, flood maps will be created to determine the water level and potential inundated ruins of Teos. In order to generate maps for vulnerable areas and infrastructure elements in Teos Ancient City, impact status of risk factors and flood hazard maps will be examined on ArcMap.

#### *2.1.6 Earthquake Risk Assessment*

Turkey is a country where active fault lines and tectonic movements are intense.

> *Onat et al. (2022, pp. 1-43) stated that Western Turkey has a high seismic risk due to the subduction zone of the Eastern Mediterranean. The Hellenic Arc is the most seismologically and geodynamically active region in the Alpine-Himalayan Belt. Nineteen earthquakes of M≥6 occurred between 2008 and 2017, with epicenters often located in Southern Greece and Western Anatolia and bordering the Aegean plate. In 2005, Seferihisar was shaken by a 5.9 (Mw) earthquake. The Aegean Sea region in Turkey was shaken for two months before 30 October, especially in 2020. These seismic activities were the harbinger of the main shock. On October 30, 2020, a strong (Mw=6.9) and shallow (14.9 km) earthquake struck Samos for 16 seconds. In the month following the mainshock, 5068 aftershocks occurred, resulting in 117 deaths and 1632 injuries.*

In order to express the earthquake-prone region at the same level as this earthquake, a potential ground motion activity map was created in Figure 2.9 and this map includes a time period of 475 years (Onat et al., 2022, p. 2).

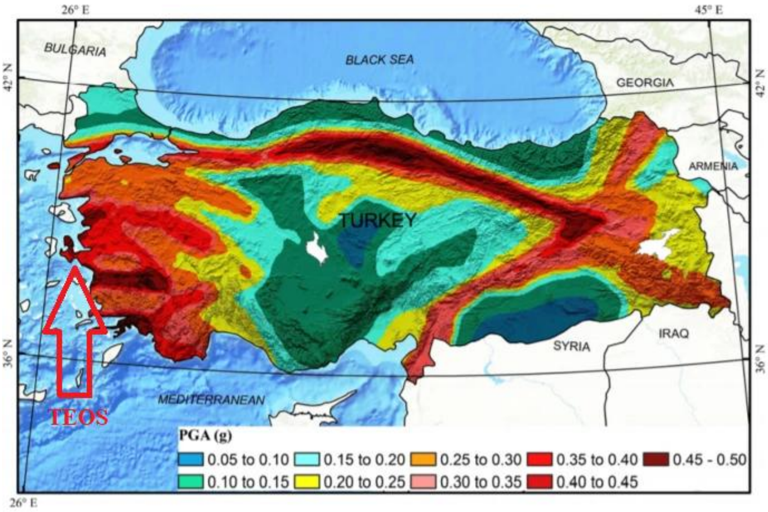


Figure 2.9 Representation of seismicity in PGA in 475 years. Adapted from (Onat et al., 2022, p. 3)

Sığacık is located in an earthquake-prone region due to the location of the fault lines.

Bakak et al. (2015, pp. 233-234) stated that Gülbahçe Fault has been the most important line in the morphological and structural separation of Izmir Bay and Karaburun Peninsula and that epicenters were formed predominantly along the southern part of the mentioned fault line. Active right-lateral strike-slip Seferihisar Fault was located between the Gulf of Sığacık and Güzelbahçe which can be seen in Figure 2.10, and this length was measured approximately as 30 km.

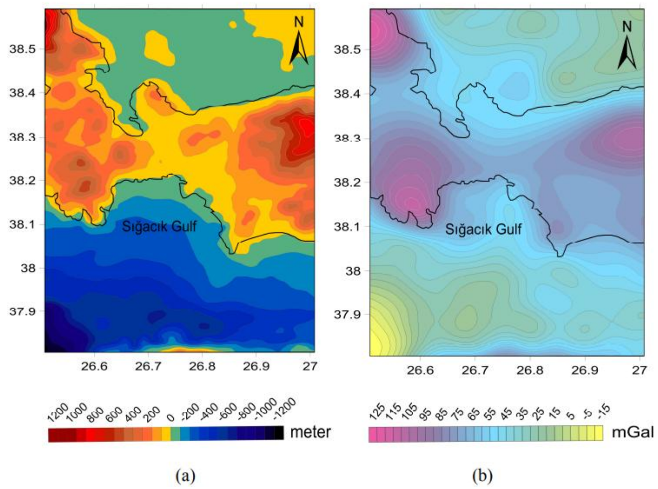


Figure 2.10 a) TOPEX topography map and b) TOPEX satellite free air gravity anomaly map (Bakak et al., 2015, p. 234)

Figure 2.11 shows areas with seismic risk and Teos located in high risk area (Zone I) (Halicioglu & Ozener, 2008, p. 4745).

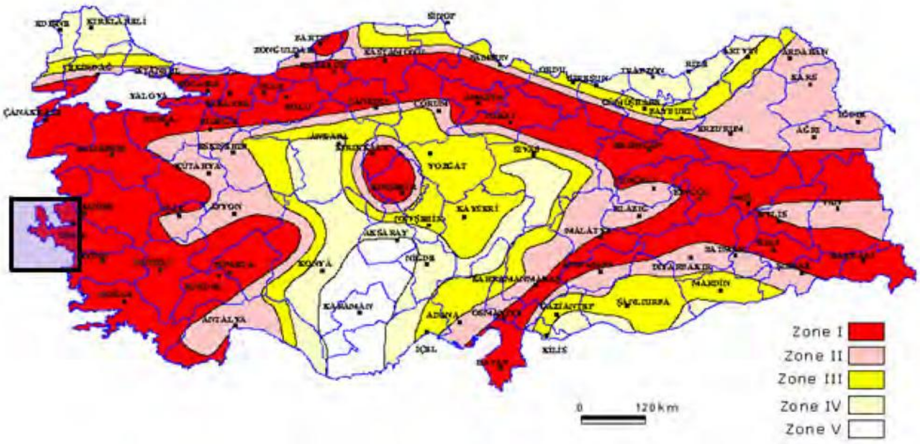


Figure 2.11 Turkey earthquake risk map and rectangle covering Teos (Halicioglu & Ozener, 2008)

Geoscience Australia (2022) explained that Interferometric Synthetic Aperture Radar (InSAR) is a useful geodetic technique that can identify movements of the Earth's surface. InSAR observations can be utilized to detect, measure, and monitor changes related to geophysical activities. When combined with ground-based geodetic monitoring, such as Global Navigation Satellite Systems (GNSS), InSAR can identify surface movements precisely.

***Working mechanism of InSAR***

According to Geoscience Australia (2022), InSAR uses two or more Synthetic Aperture Radar (SAR) images of an area to observe surface movements over a period of time. Remote sensing satellites collecting SAR images transmit pulses of microwave energy to the Earth's surface and record the amount of backscattered energy. SAR images contain information about the Earth's surface in the form of amplitude and phase components of the backscattered radar signal.

In Figure 2.12, working principle of InSAR can be observed.

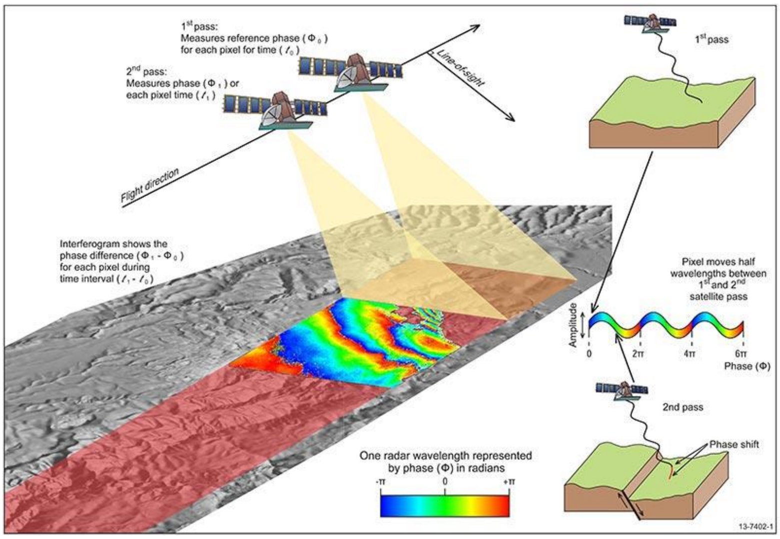


Figure 2.12 Working principle of InSAR (Geoscience Australia, 2022)

Displacements in Sığacık will be identified based on a specific earthquake that occurred in 2017.

### *2.1.7 Structural Damage Assessment*

"Light Imaging Detection and Ranging (LiDAR) can remotely detect the surface and deformation shape of structures without the need for attached sensors" (Jo et al., 2020, p. 1).

According to Olsen et al. (2010, pp. 264-265), Terrestrial Laser Scanning (TLS) has been developed to effectively model 3D objects with remote sensing.

Chen et al. (2013, p. 487) stated that 3D LiDAR is a scanning laser technology that can gather millions of optical-photonic points that contain the light diffraction and XYZ position data of each scanned point.

Chen et al. (2013, pp. 487-493) explained that LiDAR scanning effectively performs damage assessment in large structures with its speed and high resolution.

Oblique and multi-perspective imagery will be obtained. These images will be photogrammetrically analyzed and utilized to determine millimetric deformation in

Teos Ancient City.

### *2.1.8 UAV Imaging*

According to Ngadiman et al. (2018 pp. 1-6), Unmanned Aerial Vehicle (UAV) refers to a class of aircraft that can fly without the onboard presence of a pilot. Orthophotographs are produced by scanning an aerial photo diapositive, orthorectifying the digital image, and registering it to a coordinate system and map projection. Traditional methods are time consuming and costly compared to UAV so UAV has become an alternative in orthophoto map making because it is also considered time-effective. Furthermore, with user-friendly imaging software it is easy to turn images into georeferenced orthomosaic models (Ngadiman et al., 2018 pp. 1-6).

UAV flights were carried out to observe the most up-to-date status of the ruins in Teos.

### *2.1.9 Monitoring Displacements with PSI Technique*

> *Monitoring of ground deformations caused by natural processes (tectonics, subsidence or slope movements) or by anthropogenic transformation of the natural environment (groundwater exploitation, gas, oil and drilling) is a key factor to mitigate risks on civil structures and the surrounding environment. In particular, the monitoring of linear infrastructure networks is crucial for the safety of population in terms of socioeconomic resources and for the sustainability of production processes. .... In recent years, the use of a long series of continuous differential radar interferometry data has emerged as a very useful method for monitoring slow-moving landslides that can lead to damage of structures. The SAR technique can be used to analyze the static behavior of civil structures in both disrupted (during construction or restoration work) and undisrupted conditions and can aid in damage assessment analysis and scenario-based risk assessment. .... Over the years, DInSAR deformation time series have been exploited in a wider variety of*

*geophysical contexts, such as seismic, volcanic, and mass movement scenarios, with a dual purpose: to map ground displacements and monitor them over time (D'Aranno et al., 2021, pp. 1-2).*

Displacements in Teos Ancient City will be monitored by using Persistent Scatterer Interferometry (PSI) Technique as an alternative for LiDAR surveys.

## 2.2 Analytic Hierarchy Process (AHP)

Saha et al. (2021, p. 6) stated that Analytical Hierarchy Process (AHP) is a common and subjective method that includes many criteria and helps to decide by determining the weights of the criteria when it is necessary to decide between these criteria.

Goepel, (2017, p. 1) has developed a web-based, free of charge AHP online system that allows comparison of decision criteria and analysis to aid decision making. The software can compute group concurrence based on Shannon α and β-entropy and estimate weight uncertainties based on random small variations that come from judgements the user enters.

The mentioned Analytic Hierarchy Process system (AHP-OS) which can be found online and free of charge will be used to determine the order of importance of risk factors.

# CHAPTER 3
# MATERIALS AND METHOD

Satellite images and software used to analyze the risk factors mentioned in the introduction are shown in the tables below (Table 3.1 & Table 3.2).

The reason why satellite images of different dates and resolutions were used was due to the fact that the risk analyzes to be made have different contents.

The materials mentioned within the scope of "service acquisiton" were covered by the "Department of Scientific Research Projects at Dokuz Eylül University" since the thesis was evaluated as a scientific research.

Table 3.1 Satellite images used for risk evaluation studies. Table made by the data obtained from (ESA, n.d.-a; ESA, n.d.-b)

| **Image** | **Date** | **Resolution** | **Usage** | **Obtained from** |
|---|---|---|---|---|
| SPOT – 6 | 2013 | Panchromatic: 1.5 m at nadir<br>Multispectral: 6 m at nadir | Supervised Classification Analysis | İTÜ UHUZAM (https://web.cscrs.itu.edu.tr) |
| SPOT – 6 | 2020 | Panchromatic: 1.5 m at nadir<br>Multispectral: 6 m at nadir | Supervised Classification Analysis | İTÜ UHUZAM (https://web.cscrs.itu.edu.tr) |
| Sentinel - 1 | 2017 | High: 10m/px for IW and 25m/px for EW Medium: 40m/px for IW and EW | Earthquake Risk Assessment | Copernicus Sentinel data 2015, processed by European Space Agency (https://www.esa.int/) |

Table 3.1 continues

| | | | | |
|---|---|---|---|---|
| Ortophoto Image | 1957 | 0.74x0.93 cm | Defining Proximity to Transportation Routes | General Directorate of Mapping (https://www.harita.gov.tr) |
| Ortophoto Image | 1986 | 0.22cmx0.28cm | Defining Proximity to Transportation Routes | General Directorate of Mapping (https://www.harita.gov.tr) |
| Ortophoto Image | 2020 | 0.22cmx0.28cm | Defining Proximity to Transportation Routes | General Directorate of Mapping (https://www.harita.gov.tr) |
| UAV Image | 2021 | Service acquisition | Structural Damage Assessment | Department of Scientific Research Projects at Dokuz Eylül University |
| Lidar Image | 2021 | Service acquisition | Structural Damage Assessment | Department of Scientific Research Projects at Dokuz Eylül University |

The software used in the risk analysis covering the work area are shown in Table 3.2.

Table 3.2 Software used for risk evaluation studies

| **Software** | **Usage** | **Obtained from** |
|---|---|---|
| IDRISI | - Supervised Classification Analysis | GIS laboratory of The Graduate School of Natural and Applied Sciences at Dokuz Eylül University(https://fbe.deu.edu.tr/) |

Table 3.2 continues

| | | |
|---|---|---|
| ArcMap | - Defining Proximity to Transportation Routes<br>- Soil Erosion Risk Analysis<br>-Watershed Risk Assessment<br>- Coastal Flood Risk Analysis | GIS laboratory of The Graduate School of Natural and Applied Sciences at Dokuz Eylül University (https://fbe.deu.edu.tr/) |
| The Sentinel Application Platform (SNAP) | - Earthquake Risk Assessment | ESA (https://www.esa.int/) |
| Service acquisition | - UAV Imaging | Department of Scientific Research Projects at Dokuz Eylül University |

## 3.1 Exploratory Factor Analysis

The representation of natural and human-induced measurable risk factors threatening the ancient city of Teos with their inputs can be found in the table below (Table 3.3).

Table 3.3 Representation of natural and human-induced measurable risk factors

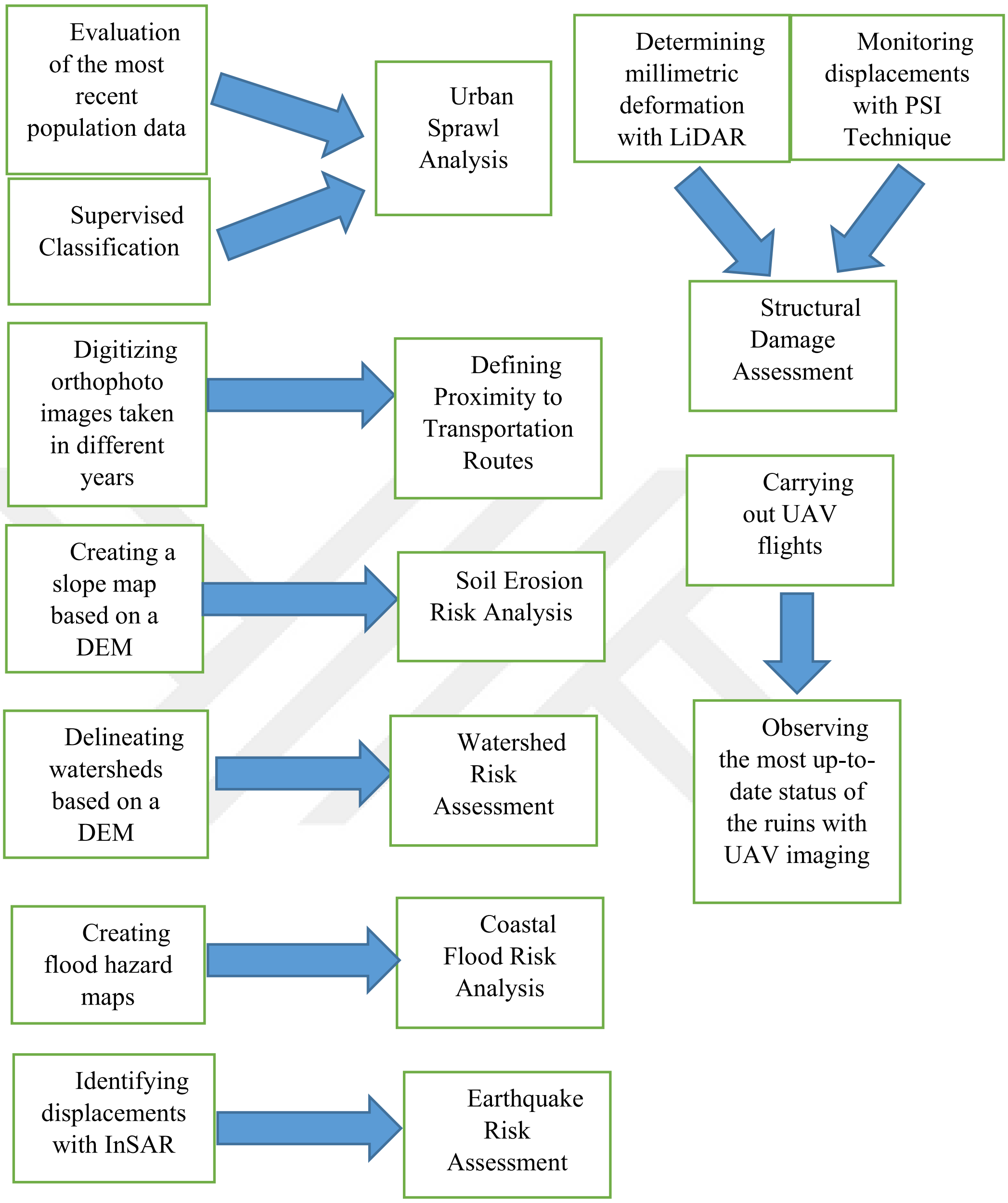

### *3.1.1 Urban Sprawl Analysis*

The studies to monitor and explore anthropogenic hazard risks in Teos Ancient City consist of urban sprawl which is the the rapid geographic growth of cities and towns. By making this analysis, urban growth in the study area can be determined.

Another study to analyze the anthropogenic risk in Teos was compromised of defining proximity to transportation routes. Accessibility to transportation routes is seen to be a major factor in urbanization.

It is important to perform these two analyzes in order to accurately assess the anthropogenic impact.

Urban sprawl can also be demonstrated with official statistical data. These data show the numerical increase in the urban sprawl in the region over the years (Fig. 2.3 & Fig. 2.4).

#### *3.1.1.1 Supervised Classification Analysis*

Another way to monitor the urban sprawl can be realized by land use/land change observation which can be determined by making supervised classification analysis. This analysis was carried out in accordance with the basis of comparing the change of classes in the satellite images obtained on two different dates based on the flow chart which consists of acquiring satellite images, enhancing and classifying them (Fig. 3.1).

Satellite image classification was implemented according to the CORINE Land Cover nomenclature. The classes covering the study area were observed as "continuous urban fabric, pastures, meadows and other permanent grasslands, annual crops associated with permanent crops, bare rock and sea".

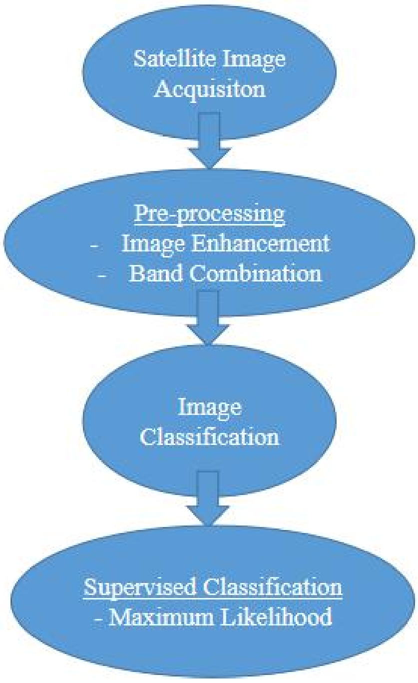


Figure 3.1 Flow chart of supervised classification analysis

SPOT-6 images from 2013 and 2020 were acquired to create training areas and signature files for image classification (Fig. 3.2 & Fig. 3.3).


Figure 3.2 SPOT-6 image taken in 2013 of Teos Ancient City and Seferihisar


Figure 3.3 SPOT-6 image taken in 2020 of Teos Ancient City and Seferihisar

Acquired SPOT-6 images were enhanced. For each class, polygons as training sites were chosen across the images. All of the drawn polygons were merged into their respective class. Signature files were created. Finally, maximum likelihood classification was realized which created an image that includes the colors for each class based on the CORINE Land Cover nomenclature and the images were classified (Fig. 3.4 & Fig. 3.5)

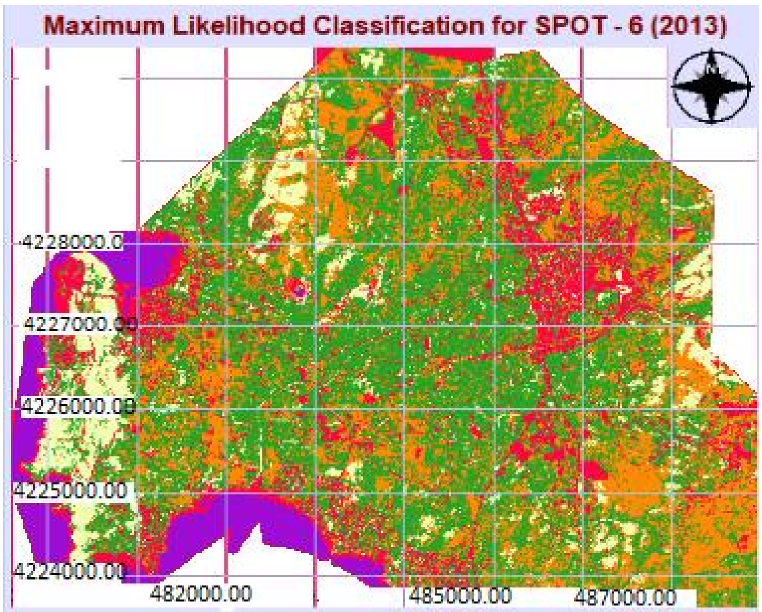


Figure 3.4 Maximum likelihood classification for SPOT-6 image taken in 2013

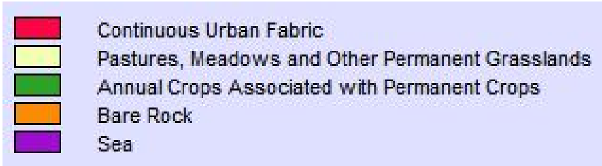


Figure 3.4 continues

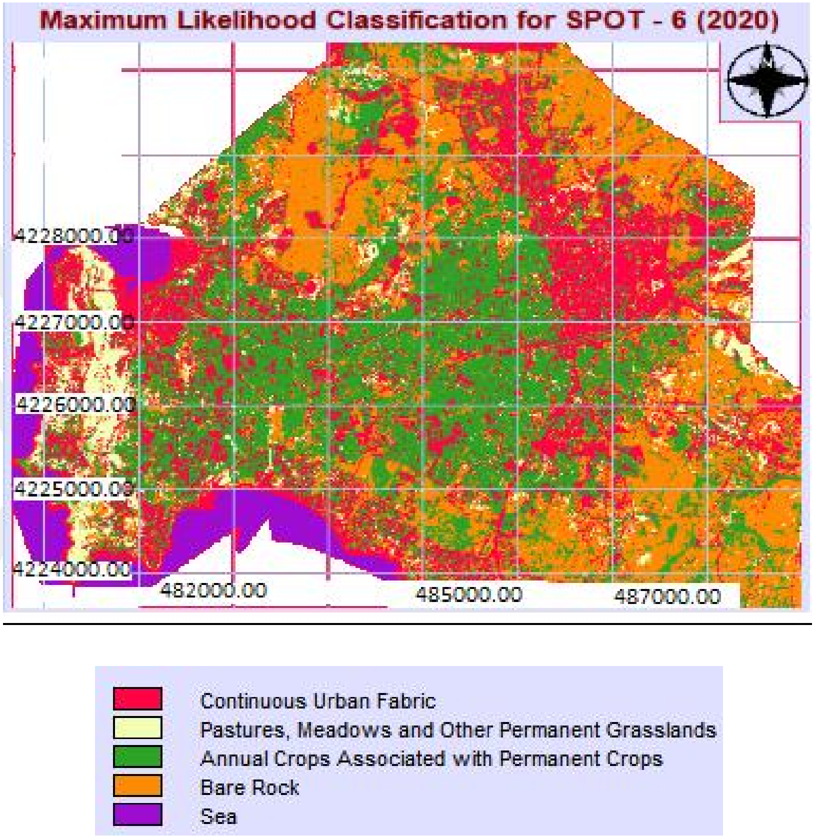


Figure 3.5 Maximum likelihood classification for SPOT-6 image taken in 2020

### *3.1.2 Defining Proximity to Transportation Routes*

Road network in Sığacık town and in Seferihisar district were analyzed in 1957, 1986 and 2020 using digital ortophoto images in order to observe the variation of the total path length in the study area with time.

Initially, new shapefiles as polylines were created using ArcMap software. Spatial reference of the digital ortophoto images were imported. All of the the paths were digitized. The separate digitized lines were merged and they became one single line so that the total length of the routes for each year was calculated (Fig. 3.6, Fig. 3.7 & Fig. 3.8).

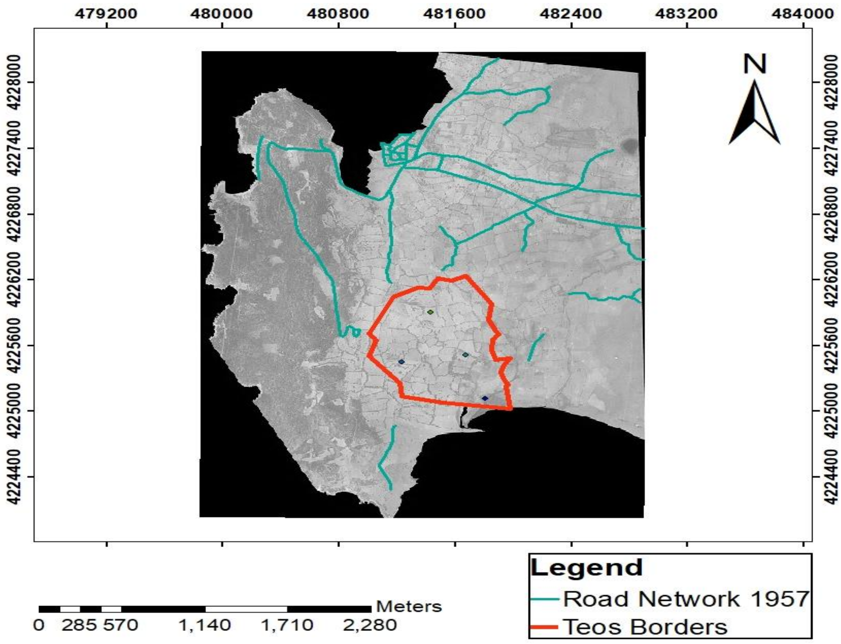


Figure 3.6 Road network in Sığacık town and in the center of Seferihisar in 1957

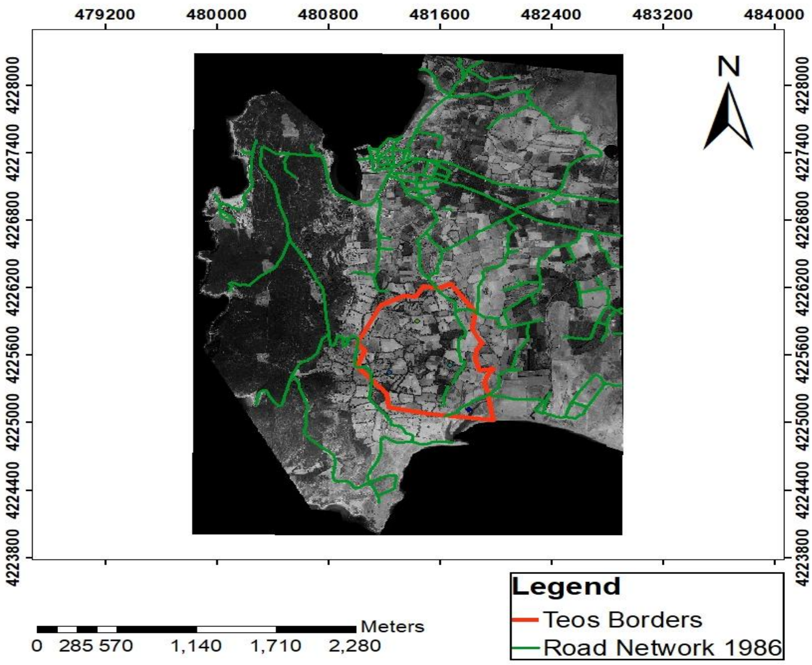


Figure 3.7 Road network in Sığacık town and in the center of Seferihisar in 1986

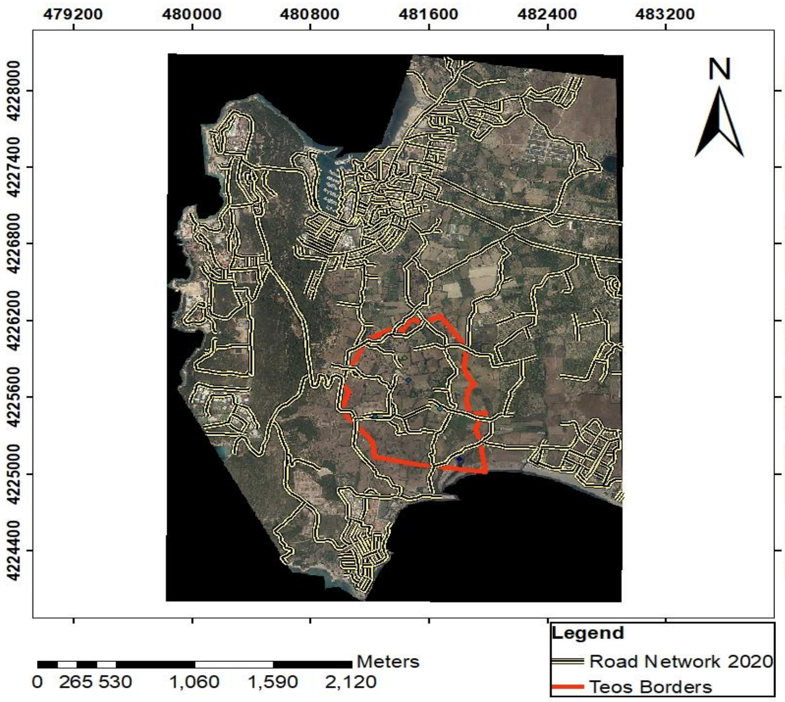


Figure 3.8 Road network in Sığacık town and in the center of Seferihisar in 2020

### *3.1.3 Soil Erosion Risk Analysis*

In order to analyze soil erosion, one of the natural risks threatening Teos Ancient City, a slope map was created using the Digital Elevation Model (DEM).

DEM of Teos was obtained from the contour layer using Google Earth data from 2020. In the next step, the slope map was obtained from Digital Elevation Model using "Slope" tool on ArcMap software (Fig. 3.9).

Places with a higher percentage of slope on the slope map have a higher risk of soil erosion.

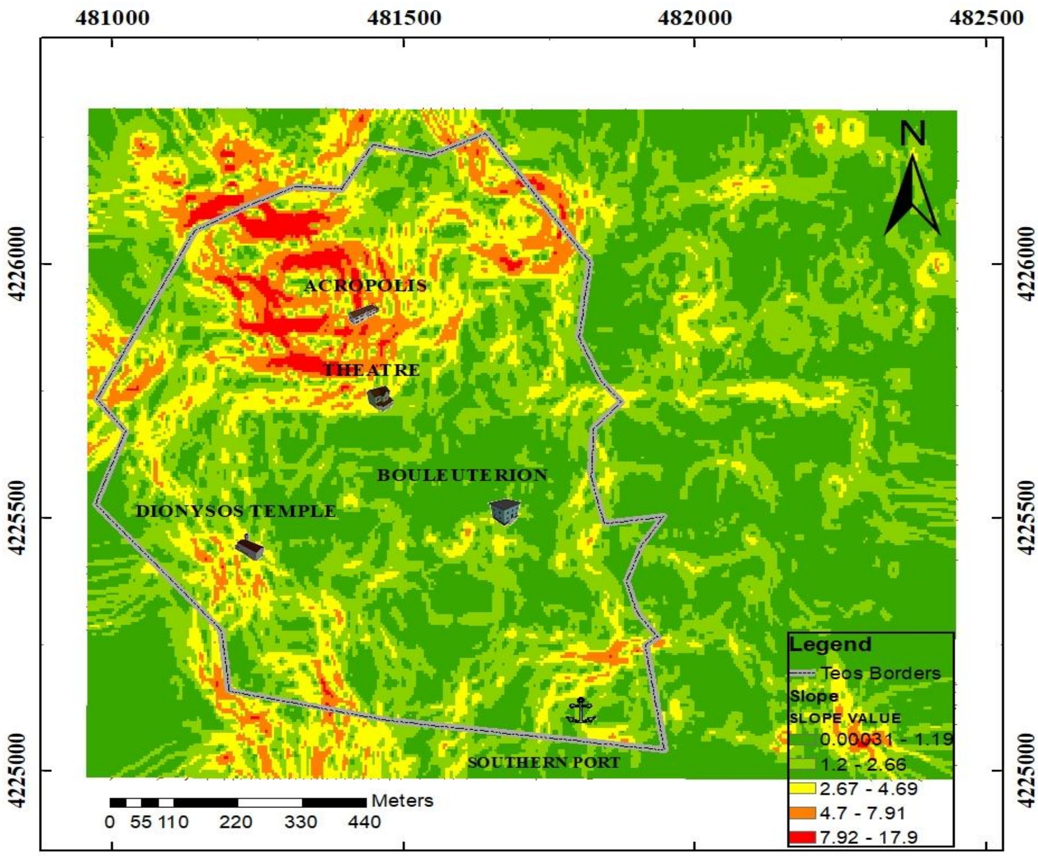


Figure 3.9 Slope map of Teos Ancient City

### *3.1.4 Watershed Risk Assessment*

A watershed analysis was carried based on the flow chart (Fig. 3.10) to reveal the basins in the study area and to identify possible risks.

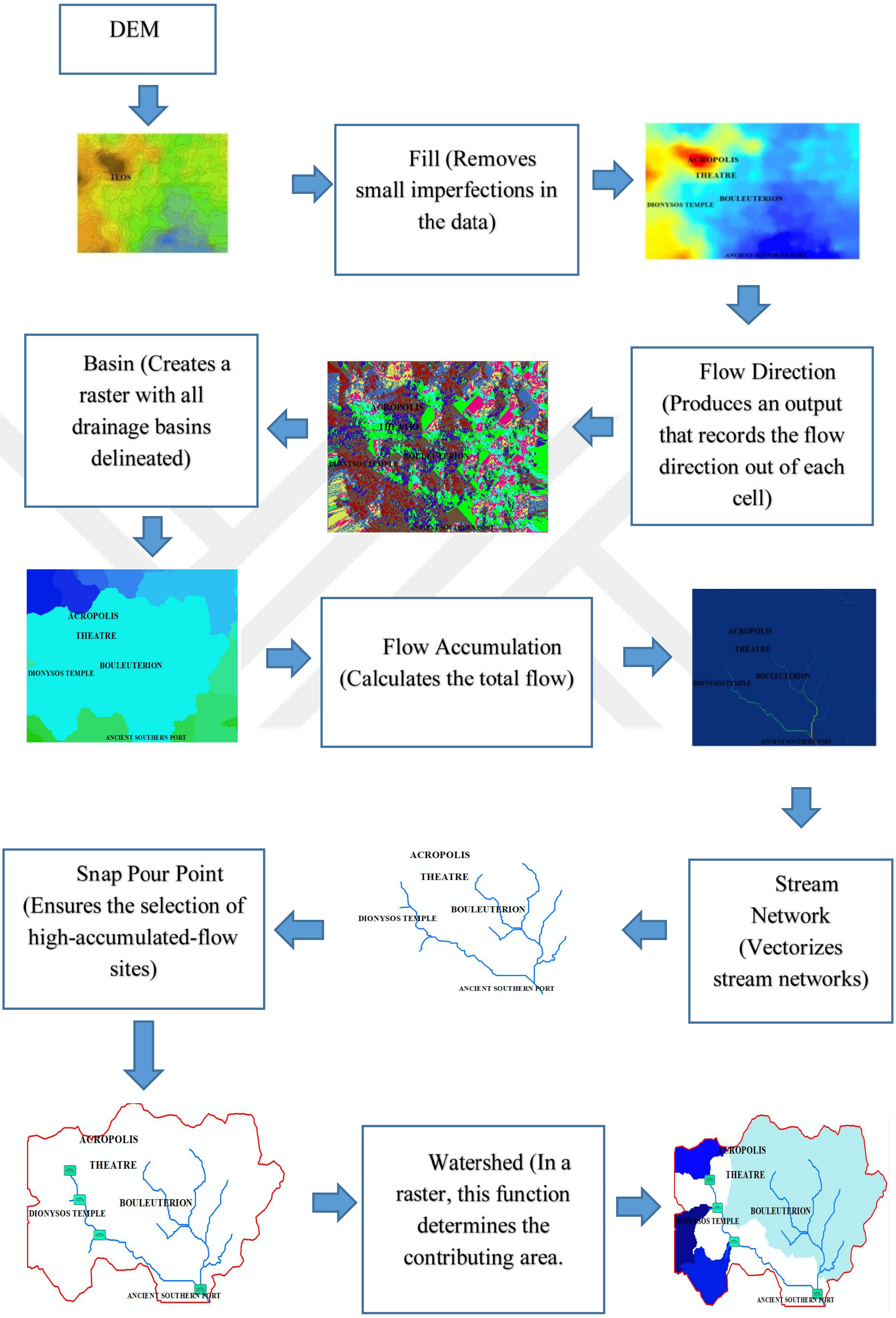


Figure 3.10 Flow chart for delineating a watershed

A Digital Elevation Model (Fig. 3.11) was created to delineate the watersheds in the study area.

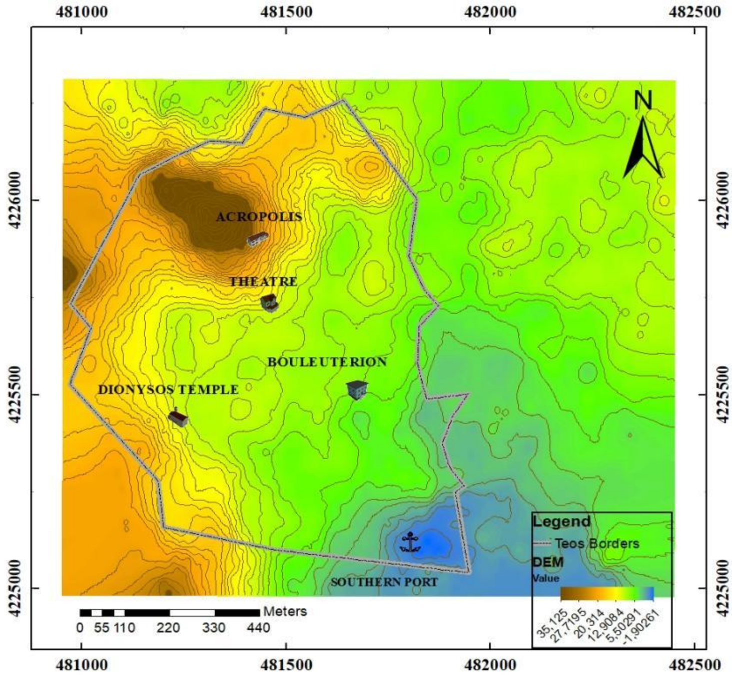


Figure 3.11 Flow chart for delineating a watershed

“Fill” tool was used to remove imperfections or sinks on the raster (Fig. 3.12).

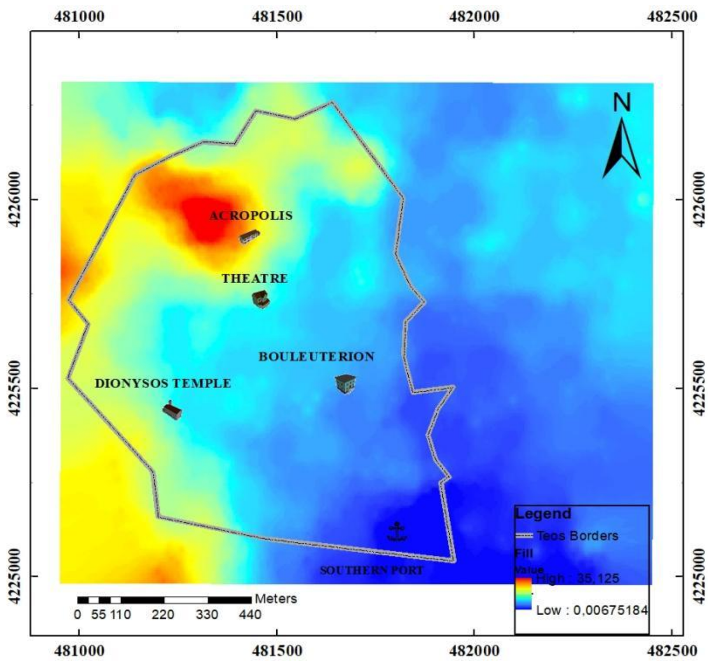


Figure 3.12 Small imperfections in the data were removed using Fill tool

Then “Flow Direction” tool was used to determine the direction which water would flow out of each cell (Fig. 3.13)

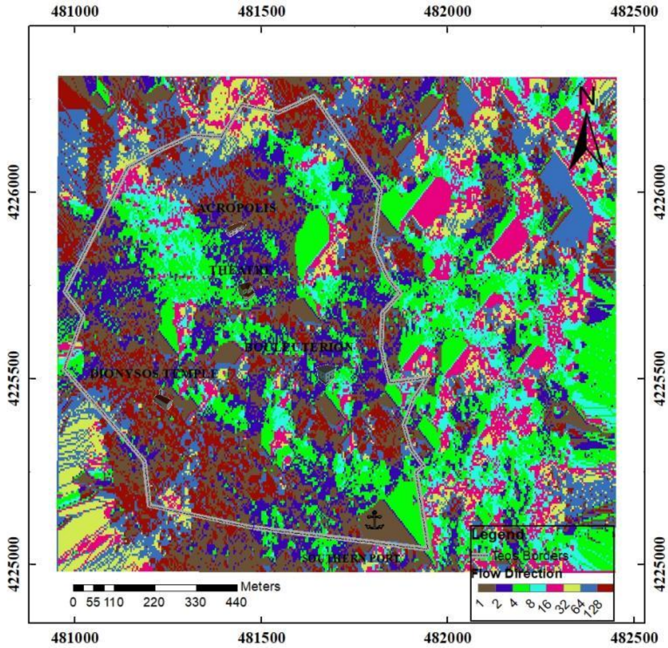


Figure 3.13 Flow direction analysis of the study area

“Basin” tool was used to create a raster delineating all drainage basins (Fig. 3.14)

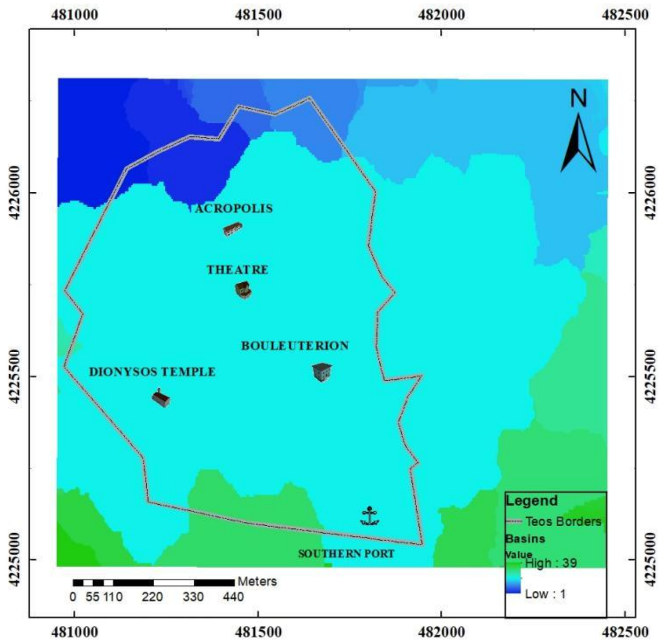


Figure 3.14 Delineated watersheds in the study area

The result raster of basin was transformed into the vector polygon (Fig. 3.15)

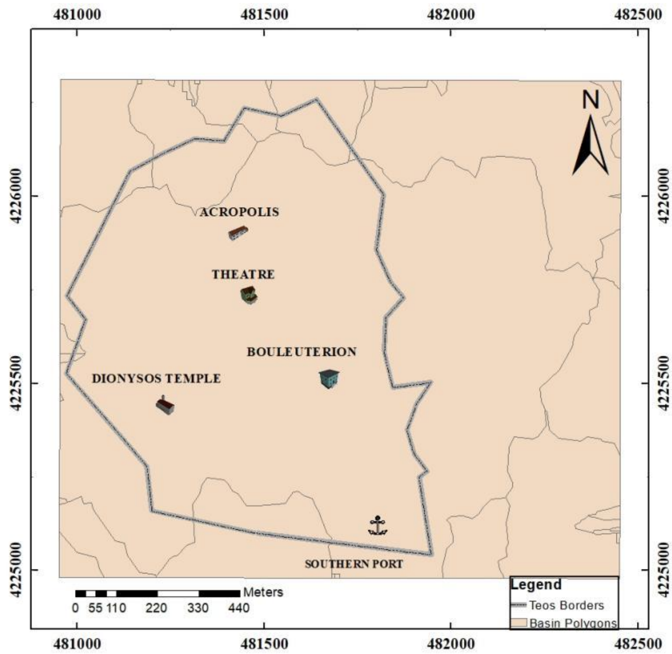


Figure 3.15 Basin polygons in the study area

Basin polygon was chosen and the chosen basin was cut from the rest of the basin polygons (Fig. 3.16).

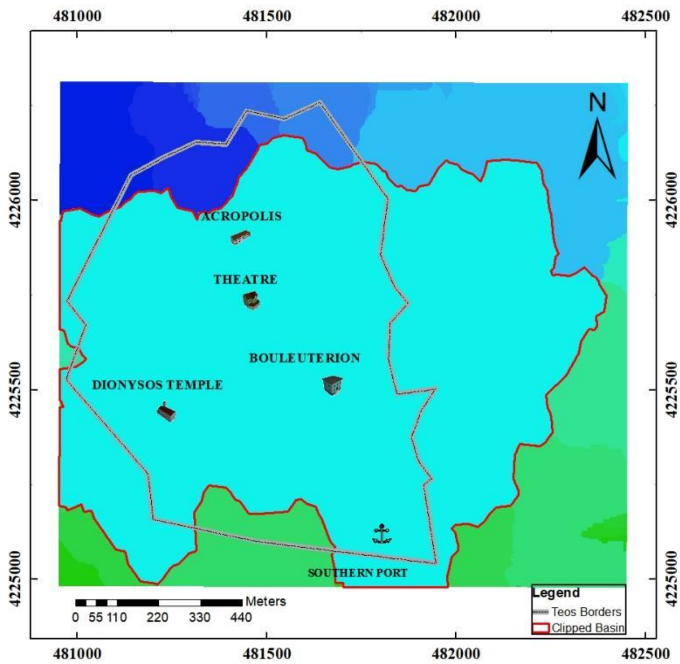


Figure 3.16 Clipped basin

Subsequently "Flow accumulation" tool was used to calculate the number of upslope cells flowing to a location (Fig. 3.17)

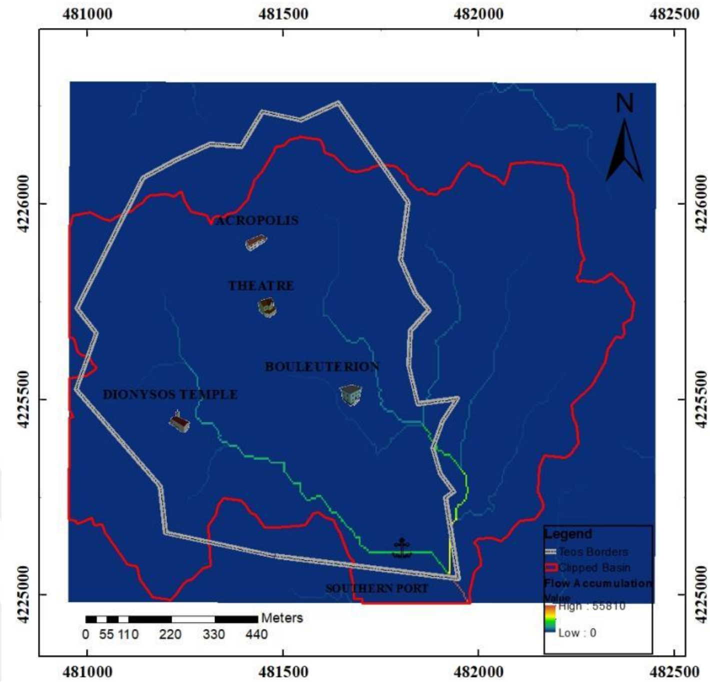


Figure 3.17 Flow accumulation analysis

"Raster Calculator" tool was used to define the stream network system. The accumulation value was set greater than 2,500 which means all cells with more than 2,500 cells flowing into them would be part of the stream network. This value depends on the size of the pixel and the raster. "Raster to Polyline" tool was used in order to transform the stream network raster to a polyline layer (Fig. 3.18).

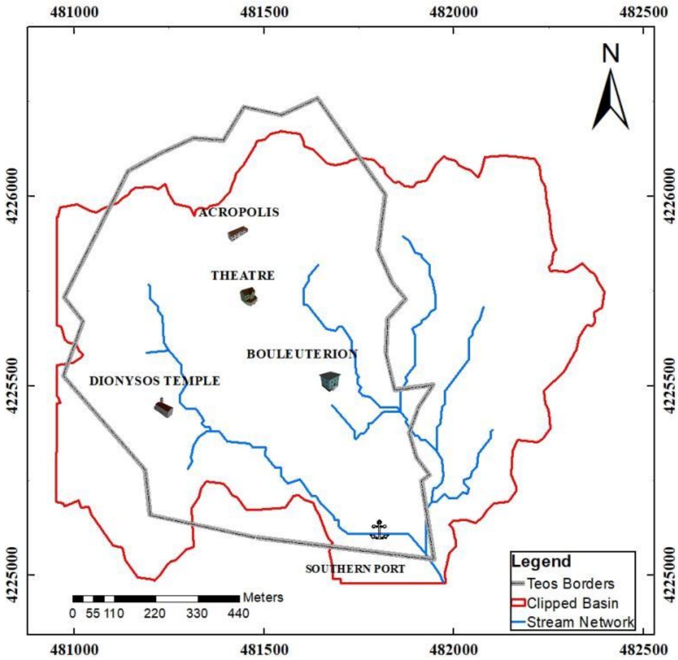


Figure 3.18 Stream network in Teos Ancient City

DEM was clipped based on the selected basin. Finally, based on the study area, 5 pour points were chosen according to the proximity status of each ruin to delineate the watersheds (Fig. 3.19)

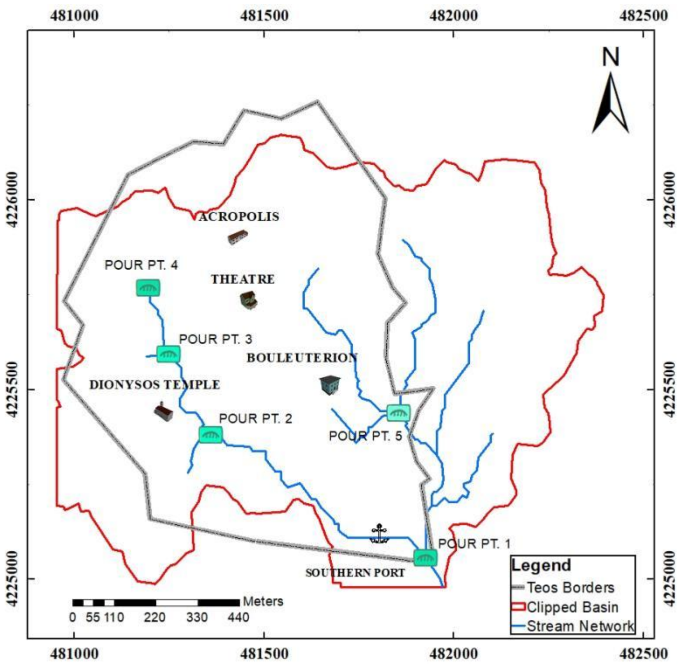


Figure 3.19 Chosen pour points in the study area

Finally, based on the chosen pour points, watersheds were delineated (Fig. 3.20).

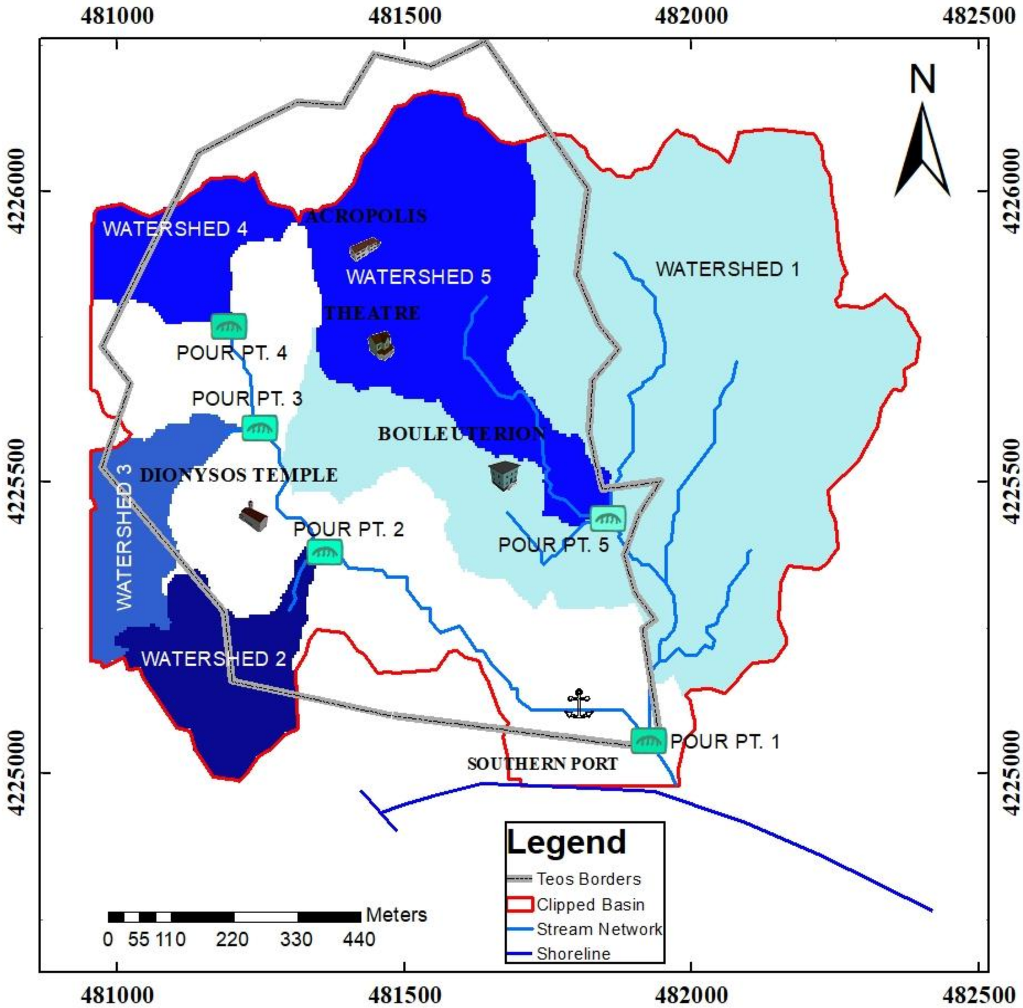


Figure 3.20 Delineated watersheds in the study area

### *3.1.5 Coastal Flood Risk Analysis*

Sea levels of 1m, 3.8m and 5m were selected as a result of the tsunami observed after the earthquake with a magnitude of Mw 6.9 on October 30, 2020, which greatly affected İzmir and Seferihisar. Coastal flood risk analysis was realized to evaluate the possible impact in case of a larger earthquake or another natural hazard likely to result in a tsunami.

“Reclassify” tool was used in order to modify the values in the raster using user-defined values of 1m, 3.8m and 5m (Fig. 3.21, Fig. 3.22 & Fig. 3.23).

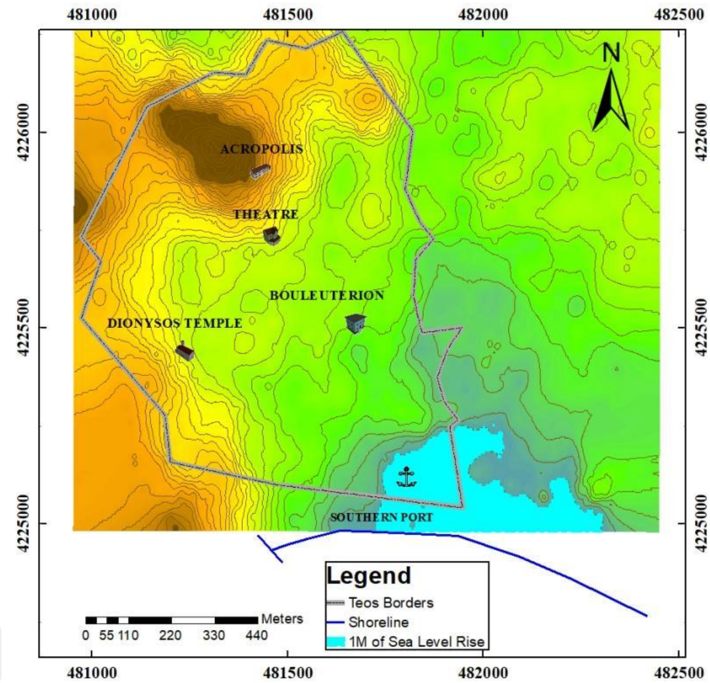


Figure 3.21 Coastal flood risk in case of a 1m. of sea level rise

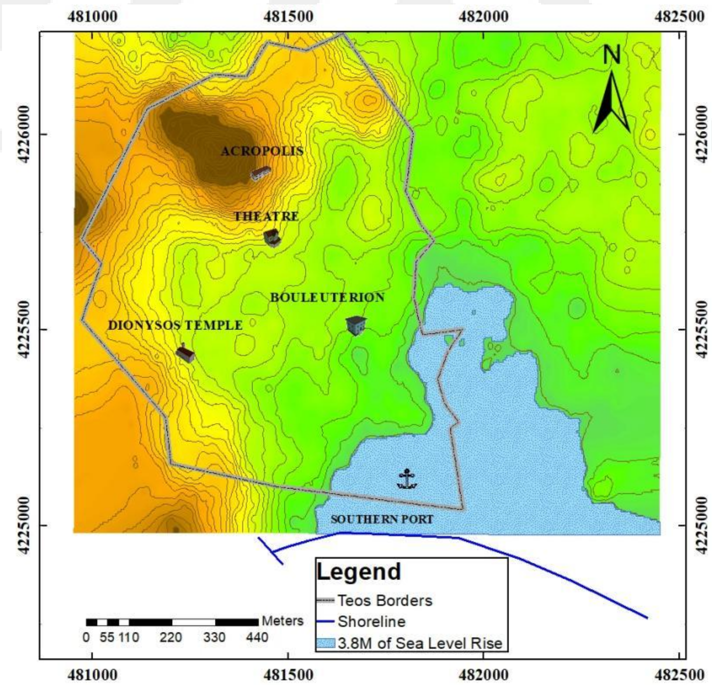


Figure 3.22 Coastal flood risk in case of a 3.8m. of sea level rise

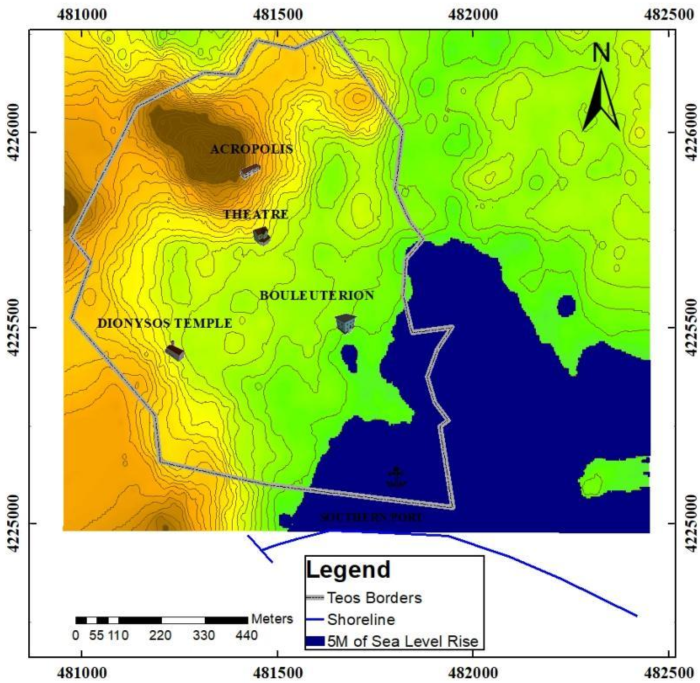


Figure 3.23 Coastal flood risk in case of a 5m. of sea level rise

### *3.1.6 Earthquake Risk Assessment*

Synthetic aperture radar interferometry was applied to create a displacement map to measure the topography of the surface and its changes over time (before and after the earthquake that occurred on 12.05.2017 in the Gulf of Kuşadası).

Satellite images (Sentinel-1) were acquired on two different dates (07.05.2017 and 13.05.2017) to produce co-seismic interferograms and observe post-seismic deformation due to the earthquake that occurred on 12.05.2017 in the Gulf of Kuşadası. The Sentinel Application Platform (SNAP), which is free of charge, was used to perform differential interferometric processing of two Single Look Complex (SLC) data (Fig. 3.24).

The processing steps of Interferometric Synthetic Aperture Radar (InSAR) analysis for two selected Sentinel-1 satellite images can be found as coregistration, interferogram formation, deburst, topographical phase removal, phase filter, unwrapping, and phase to displacement.

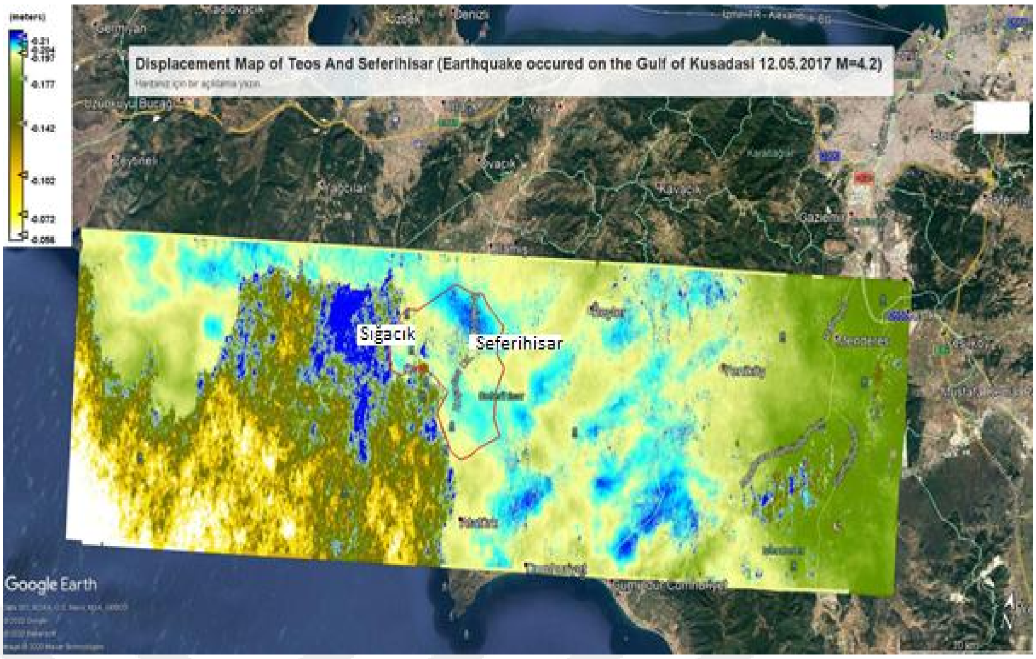


Figure 3.24 Displacement map after applying InSAR

### *3.1.7 Structural Damage Assessment*

Terrestrial LiDAR scanner was planned to be used in order to detect millimetric changes in the structures between two different dates. However, because of the pandemic conditions and the lack of economic funding, second measurements could not be realized.

LiDAR outputs obtained as a result of the first measurement are 2 pieces (Fig. 3.25 & Fig. 3.26). In the 2nd output image (Fig. 3.26), vegetation has been removed for more accurate LiDAR studies.

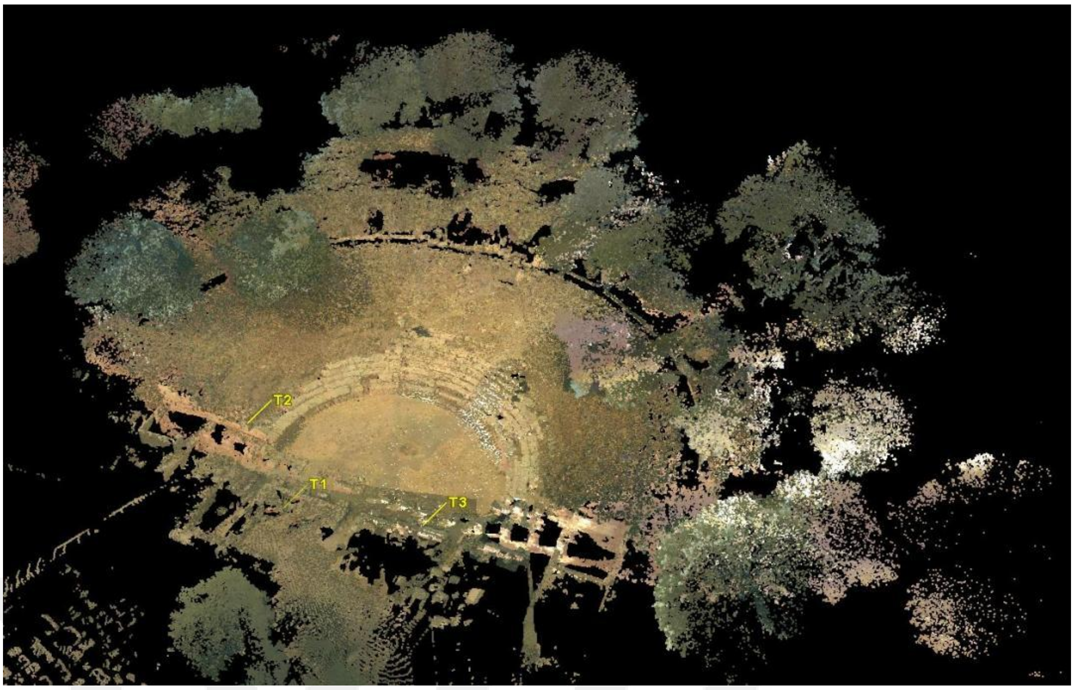

Figure 3.25 Terrestrial LiDAR output image in the study area

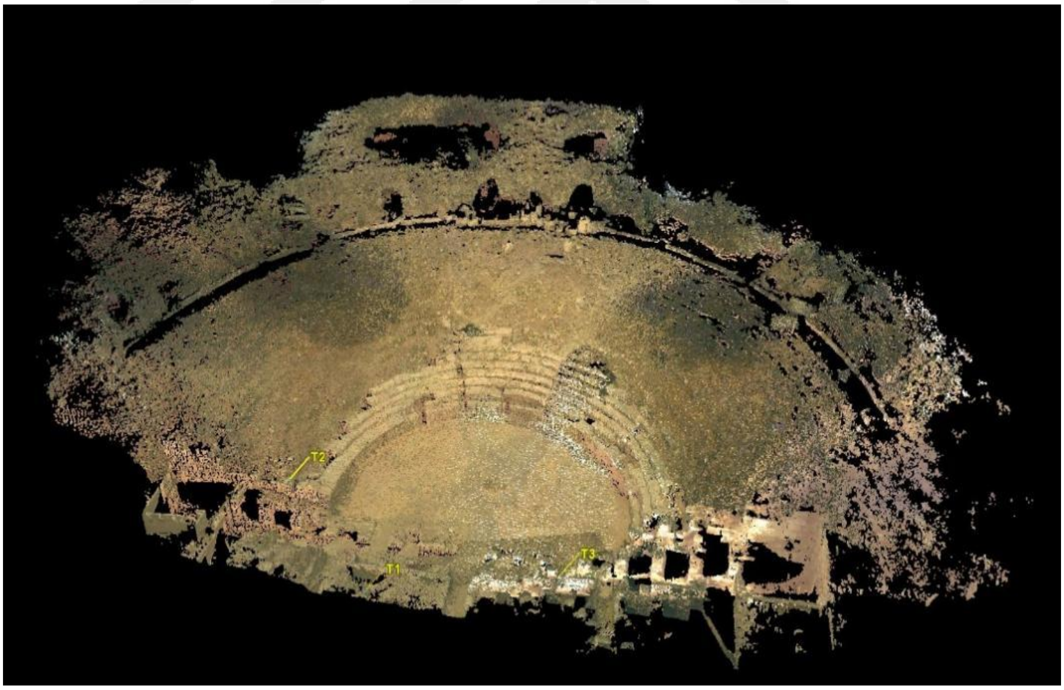

Figure 3.26 Terrestrial LiDAR output image in the study area without vegetation

### *3.1.8 UAV Imaging*

The UAV images were used to produce the most up-to-date map of the study area (Fig. 3.27).

The UAV flights included oblique picture acquisition and were pre-planned using modern UAV systems' waypoint capability.


Figure 3.27 UAV image of Teos made with UAV flight outputs in 2021

In addition, the most up-to-date UAV images of the important ruins in Teos were obtained during the UAV flights (Fig. 3.28, Fig. 3.29, Fig. 3.30, Fig.3.31 & Fig. 3.32)

Figure 3.28 UAV image taken in 2021 that shows Acropolis

Figure 3.29 UAV image taken in 2021 that shows Theatre

Figure 3.30 UAV image taken in 2021 that shows Dionysus Temple

Figure 3.31 UAV image taken in 2021 that shows Bouleuterion

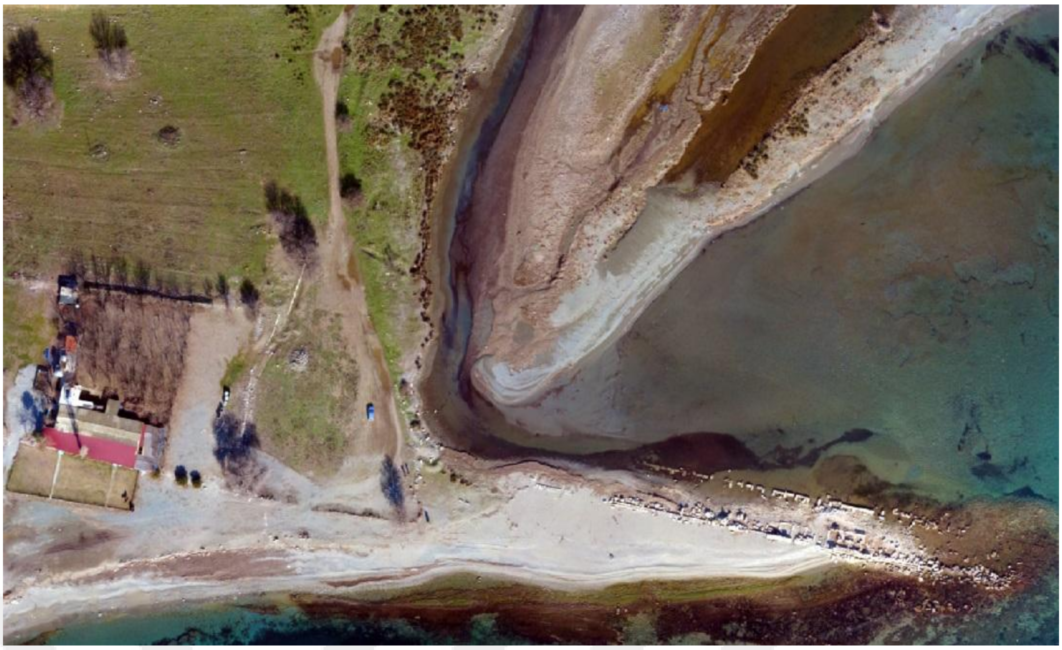

Figure 3.32 UAV image taken in 2021 that shows Southern Port

## 3.2 Analytic Hierarchy Process (AHP)

An online software called *AHP Online System - AHP-OS* developed by *Klaus D. Goepel, BPMSG* which works based on the AHP Statistics technique was used for evaluating all the risk analysis results together and to compare each risk factor with the others. In determining the order of importance of risk factors relative to each other, besides my personal views, the views of my thesis advisor Asst. Prof. A. Hüsnü Eronat and Assoc. Prof. Fethi Bengil were also used.

If the influence of two criteria was the same or had equal importance, a score of 1 was given and a score of 9 was given when the influence of one criterion was extreme over another criterion in the comparison table that was adapted from Goepel, K.D. (2018) in which the scale was defined as 1- Equal Importance, 3- Moderate importance, 5- Strong importance, 7- Very strong importance, 9- Extreme importance (2,4,6,8 values in-between). After normalizing each value by dividing the actual value to its sum of column value, weights were derived by arithmetic mean method by using the software.

# CHAPTER 4
# RESULTS

The results obtained after the analysis of each risk factor are presented under the respective headings.

### *Urban Sprawl Analysis*

Population change, which is a part of urban sprawl, was observed according to official statistical data (Fig 2.3 & Fig. 2.4).

As an alternative perspective to official statistical population data, obtained SPOT-6 images from 2013 and 2020 were subjected to Supervised Classification Analysis (Fig. 3.4 & Fig. 3.5), thus the values of each class in km² were revealed (Table 4.1 & Table 4.2).

Table 4.1 Areas (in km²) for each class after maximum likelihood classification for SPOT - 6 image taken in 2013

**Area on file: 2013MAXLIKE**

| Category | Square kilometers | Legend |
|---|---|---|
| 1 | 18.907531 | Continuous Urban Fabric |
| 2 | 4.362215 | Pastures, Meadows and Other Permanent Grasslands |
| 3 | 18.713948 | Annual Crops Associated with Permanent Crops |
| 4 | 11.556367 | Bare Rock |
| 5 | 3.133728 | Sea |

Table 4.2 Areas (in km²) for each class after maximum likelihood classification for SPOT - 6 image taken in 2020

**Area on file: 2020MAXLIKE**

| Category | Square kilometers | Legend |
|---:|---:|---:|
| 1 | 24.116477 | Continuous Urban Fabric |
| 2 | 2.870912 | Pastures, Meadows and Other Permanent Grasslands |
| 3 | 13.800245 | Annual Crops Associated with Permanent Crops |
| 4 | 12.719576 | Bare Rock |
| 5 | 3.166578 | Sea |

***Defining Proximity to Transportation Routes***

After digitizing orthophoto images from 1957, 1986 and 2020 (Fig. 3.6, Fig. 3.7 & Fig. 3.8), the total path length in the study area for each year was calculated. In 1957, the total length of roads was 23.13 km. The total road length increased by 1.8 times and reached 41.63 km in 1986. Compared to 1986, the total road length increased by 1.9 times and reached 79.10 km in 2020 (Table 4.3).

Table 4.3 Total road length (km) by year

| **Year** | **Total Path Length (km)** |
|:---:|:---:|
| 1957 | 23.13 |
| 1986 | 41.63 |
| 2020 | 79.10 |

### *Soil Erosion Risk Analysis*

After the slope map was created (Fig. 3.9), the slope value range of each ruin was revealed (Table 4.4).

Table 4.4 Slope value range of each ruin

| Ruin | Slope Value Range (cm) |
|---|---|
| Acropolis | 7.92 -17.9 |
| Theatre | 4.70 - 7.91 |
| Dionysos Temple | 2.67 - 4.69 |
| Bouleuterion | 1.20 - 2.66 |
| Southern Port | 0.00031 - 1.19 |

According to the slope value range data obtained from the slope map, the appropriate slope level of each ruin was determined (Table 4.5). The boxes show which slope column each ruin belongs to.

Table 4.5 Soil erosion risk classes. Adapted from (Scotland's soils)

| Ruin | Almost Level Slope (1-2°) | Gentle Level Slope (2-5°) | Moderate Level Slope (5-10°) | Moderately Steep Level Slope (10-18°) | Steep Slope (18-30°) |
|---|---|---|---|---|---|
| Southern Port | $\boxed{1}$ | 2 | 3 | 4 | 5 |
| Dionysus Temple | 1 | 2 | $\boxed{3}$ | 4 | 5 |
| Bouleuterion | 1 | $\boxed{2}$ | 3 | 4 | 5 |
| Theatre | 1 | 2 | 3 | $\boxed{4}$ | 5 |
| Acropolis | 1 | 2 | 3 | 4 | $\boxed{5}$ |

### *Watershed Risk Assessment*

It was shown whether the ruins could be in the flow direction of the delineated watersheds (Fig. 3.20) that emerge according to the selected pour points (Fig. 3.19). It was also stated which watersheds could influence the ruins that are in the flow direction (Table 4.6). Dionysos Temple does not seem to be affected in any watershed but since it is located close to the stream network, it is still under the influence, although not as much as other ruins.

Table 4.6 The state of being in the direction of the watershed flow

| Ruin | The state of being in the direction of the watershed flow |
|---|---|
| Acropolis | Yes / Watershed - 5 |
| Theatre | Yes / Watershed - 5 |
| Dionysos Temple | No |
| Bouleuterion | Yes / Watershed - 1 |
| Southern Port | No |

### *Coastal Flood Risk Analysis*

Possible impact areas of the selected sea level rises of 1m, 3.8m and 5m whose visual results were shown before in Fig. 3.21, Fig. 3.22 and Fig. 3.23 are indicated in km² (Table 4.7).

Table 4.7 Possible impact areas for the selected sea level rises

| Hypothetical sea level rise (m) | Possible impact area (km²) |
|---|---|
| 1 | 0.087445 |
| 3.8 | 0.270287 |
| 5 | 0.42518 |

***Earthquake Risk Assessment***

The surface deformation outputs were shown by the interferograms generated from the InSAR study (Fig. 3.24). The following table shows the values of maximum positive and maximum negative on displacement map (Table 4.8).

Table 4.8 Maximum positive and maximum negative values on the displacement map

| | |
|---|---|
| **Maximum Positive Value (cm)** | 21 |
| **Maximum Negative Value (cm)** | 6.6 |

***Structural Damage Assessment***

The first measurements made with terrestrial LiDAR could not be completed due to Covid-19 and adverse weather conditions. No conclusion could be reached with the output images obtained (Fig. 3.25 & Fig. 3.26).

***UAV Imaging***

A map covering the ancient city of Teos and its surroundings, which was created with the data obtained after the UAV flights, was revealed (Fig. 3.27).

High resolution UAV images of all important ruins in Teos were obtained after UAV flights (Fig. 3.28, Fig. 3.29, Fig. 3.30, Fig. 3. 31 & Fig. 3.32).

***Monitoring Displacements with PSI Technique***

Output images created with the PSI technique, which allow displacement observations in and around Teos Ancient City, were obtained through personal communication with Ph.D. student Hüseyin Yaşar (Fig. 4.1 & Fig. 4.2).

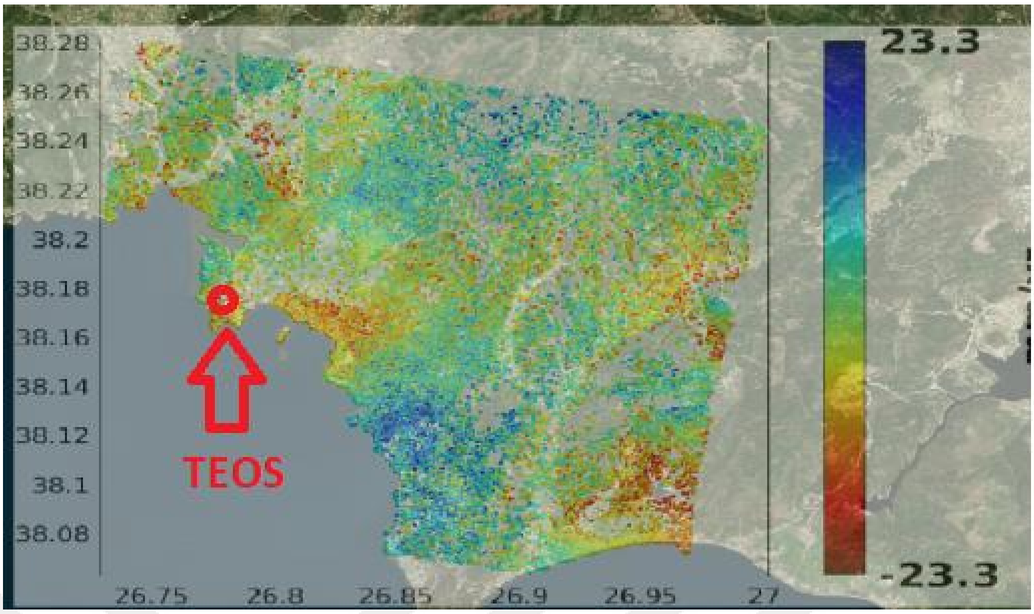

Figure 4.1. Displacement map made with PSI technique (H. Yaşar, personal communication, April 12, 2022)

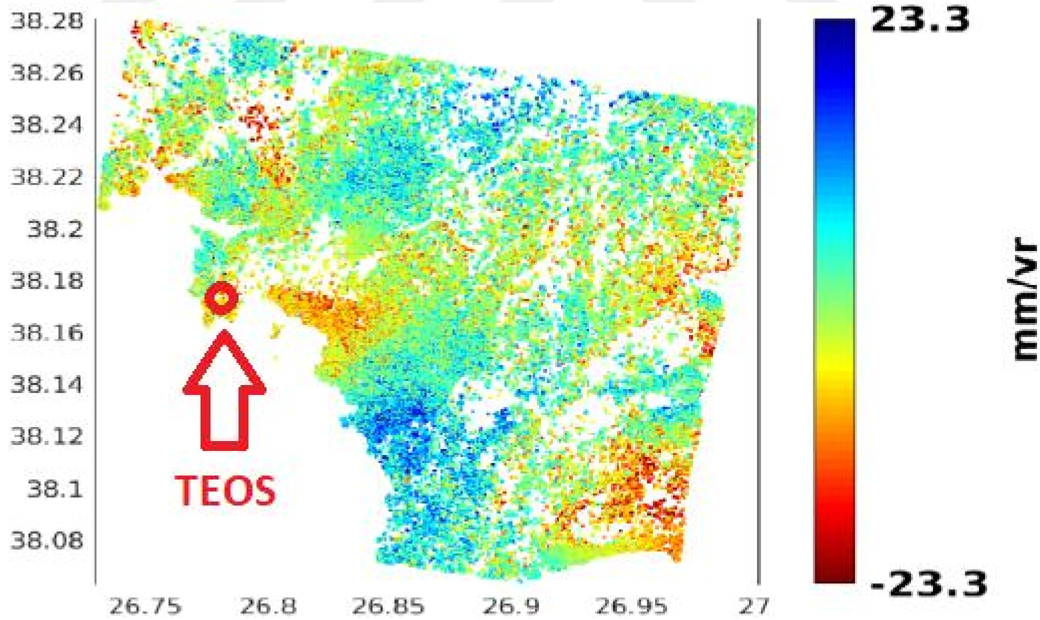

Figure 4.2. Displacement map made with PSI technique (H. Yaşar, personal communication, April 12, 2022)

***Analytic Hierarchy Process (AHP)***

As a result of the combination of my evaluation and the views of my thesis advisor Asst. Prof. A. Hüsnü Eronat and Assoc. Prof. Fethi Bengil, the comparative significance of each risk factor with each other was determined as in the table (Table 4.9).

The boxes in columns A and B indicate the risk factor being compared against the other risk factor. The boxes in the columns "equal" and "how much more" indicate how important the factor selected in column A or B is compared to the other risk factor. If the two factors are of equal importance, "equal" was selected. If the selected factor is more important than the other risk factor, the most appropriate value between 1 and 9 was chosen (Table 4.9).

Table 4.9 AHP priorities for the risk factors

| A | B | Equal | How much more? | | | | | | | |
|---|---|---|---|---|---|---|---|---|---|---|
| $\boxed{\text{Urban Sprawl}}$ | Proximity to Transportation Routes | $\boxed{1}$ | 2 | 3 | 4 | 5 | 6 | 7 | 8 | 9 |
| $\boxed{\text{Urban Sprawl}}$ | Soil Erosion | 1 | 2 | $\boxed{3}$ | 4 | 5 | 6 | 7 | 8 | 9 |
| $\boxed{\text{Urban Sprawl}}$ | Watershed | 1 | 2 | 3 | $\boxed{4}$ | 5 | 6 | 7 | 8 | 9 |
| $\boxed{\text{Urban Sprawl}}$ | Coastal Flood | 1 | 2 | 3 | 4 | $\boxed{5}$ | 6 | 7 | 8 | 9 |
| $\boxed{\text{Urban Sprawl}}$ | Earthquake | $\boxed{1}$ | 2 | 3 | 4 | 5 | 6 | 7 | 8 | 9 |
| $\boxed{\text{Urban Sprawl}}$ | Structural Damage | 1 | 2 | $\boxed{3}$ | 4 | 5 | 6 | 7 | 8 | 9 |
| $\boxed{\text{Proximity to Transportation Routes}}$ | Soil Erosion | 1 | 2 | $\boxed{3}$ | 4 | 5 | 6 | 7 | 8 | 9 |
| $\boxed{\text{Proximity to Transportation Routes}}$ | Watershed | 1 | 2 | $\boxed{3}$ | 4 | 5 | 6 | 7 | 8 | 9 |
| $\boxed{\text{Proximity to Transportation Routes}}$ | Coastal Flood | 1 | 2 | 3 | 4 | $\boxed{5}$ | 6 | 7 | 8 | 9 |
| $\boxed{\text{Proximity to Transportation Routes}}$ | Earthquake | $\boxed{1}$ | 2 | 3 | 4 | 5 | 6 | 7 | 8 | 9 |
| $\boxed{\text{Proximity to Transportation Routes}}$ | Structural Damage | 1 | 2 | $\boxed{3}$ | 4 | 5 | 6 | 7 | 8 | 9 |
| Soil Erosion | $\boxed{\text{Watershed}}$ | 1 | 2 | $\boxed{3}$ | 4 | 5 | 6 | 7 | 8 | 9 |
| $\boxed{\text{Soil Erosion}}$ | Coastal Flood | 1 | 2 | $\boxed{3}$ | 4 | 5 | 6 | 7 | 8 | 9 |
| Soil Erosion | $\boxed{\text{Earthquake}}$ | 1 | 2 | $\boxed{3}$ | 4 | 5 | 6 | 7 | 8 | 9 |
| $\boxed{\text{Soil Erosion}}$ | Structural Damage | 1 | $\boxed{2}$ | 3 | 4 | 5 | 6 | 7 | 8 | 9 |
| $\boxed{\text{Watershed}}$ | Coastal Flood | 1 | 2 | $\boxed{3}$ | 4 | 5 | 6 | 7 | 8 | 9 |
| Watershed | $\boxed{\text{Earthquake}}$ | 1 | 2 | $\boxed{3}$ | 4 | 5 | 6 | 7 | 8 | 9 |
| $\boxed{\text{Watershed}}$ | Structural Damage | 1 | 2 | $\boxed{3}$ | 4 | 5 | 6 | 7 | 8 | 9 |
| Coastal Flood | $\boxed{\text{Earthquake}}$ | 1 | 2 | $\boxed{3}$ | 4 | 5 | 6 | 7 | 8 | 9 |
| Coastal Flood | $\boxed{\text{Structural Damage}}$ | 1 | 2 | $\boxed{3}$ | 4 | 5 | 6 | 7 | 8 | 9 |
| $\boxed{\text{Earthquake}}$ | Structural Damage | 1 | 2 | $\boxed{3}$ | 4 | 5 | 6 | 7 | 8 | 9 |

As a result of the AHP analysis made with the software by Goepel, K.D. (2018), the three most important risk factors for Teos were determined as urban sprawl, proximity to transportation routes and earthquake (Table 4.10). While the number of comparisons was 21, consistency ratio was calculated as 5.4%.

Table 4.10 Weights obtained as a result of comparisons

| Cat | | Priority | Rank | (+) | (-) |
|---|---|---|---|---|---|
| 1 | Urban Sprawl | 24.5% | 1 | 9.4% | 9.4% |
| 2 | Proximity to Transportation Routes | 22.8% | 2 | 5.2% | 5.2% |
| 3 | Soil Erosion | 8.2% | 5 | 2.9% | 2.9% |
| 4 | Watershed | 12.1% | 4 | 6.6% | 6.6% |
| 5 | Coastal Flood | 4.0% | 7 | 1.5% | 1.5% |
| 6 | Earthquake | 21.8% | 3 | 6.8% | 6.8% |
| 7 | Structural Damage | 6.7% | 6 | 2.6% | 2.6% |

Percent consolidated results of all risk factors were also obtained as a result of the application (Fig. 4.3).

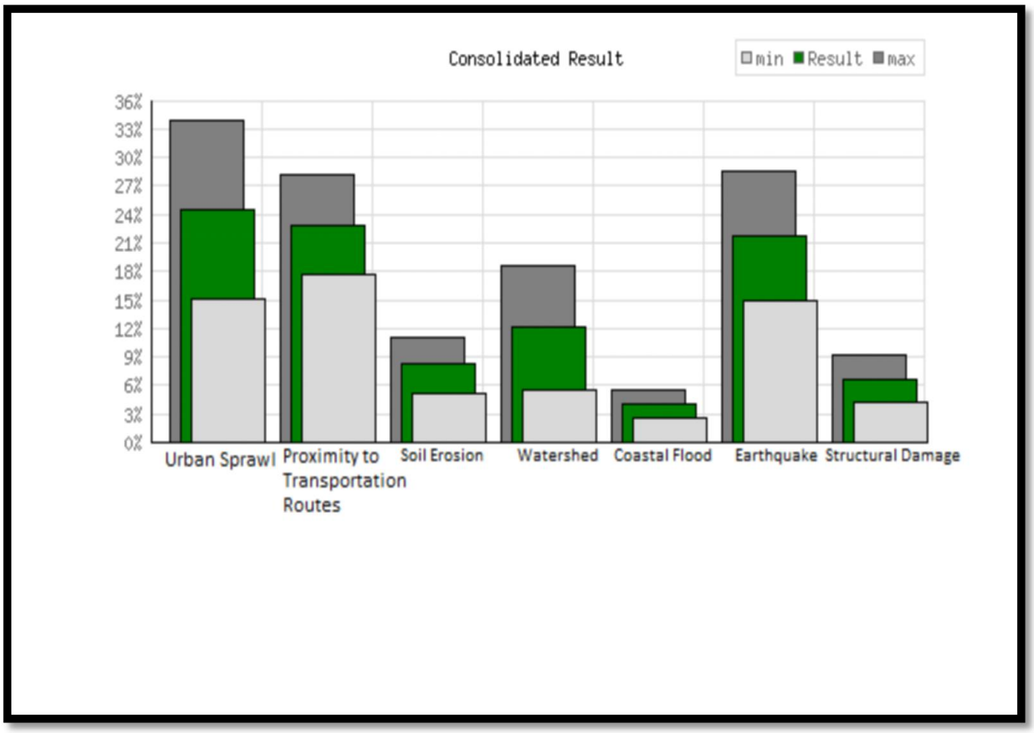


Figure 4.3. Consolidated results after AHP analysis

# CHAPTER 5
# DISCUSSION

According to the literature review, no previous study has been found in which the risk factors of any cultural heritage are discussed on such a large scale though similar results were found as Agapiou et al. (2015) stated that cultural heritage can be damaged by both human and natural hazards, and it has been understood that the most effective detection of these hazards and taking the necessary precautions are possible with remote sensing and GIS. As a result of all risk analyzes carried out in the study area, the following conclusions were reached:

- One of the main effects of population growth was seen as the increase of the urbanization rate. While urbanization rate rises, other classes such as “Annual crops associated with permanent crops” and “Pastures, meadows and other permanent grasslands” decrease evenly (Fig. 5.1).

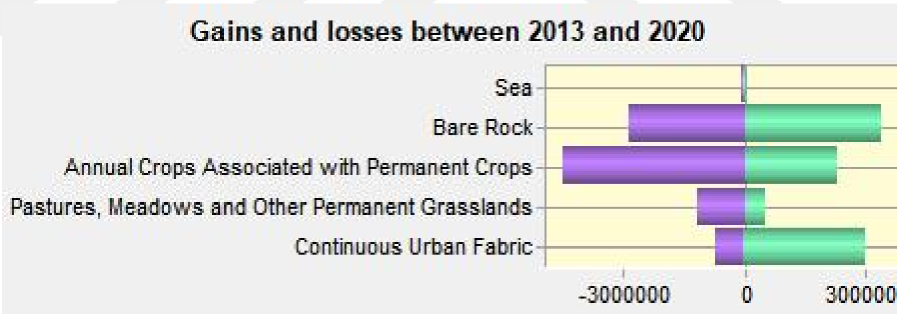


Figure 5.1. Comparison of gains and losses for each class after supervised classification analysis

- With the increase in population in the study area, more roads were needed. The paving process, making of new roads, the renewal and improvement of old roads have begun, also the paths in Teos Ancient City have been improved, allowing visitors to easily navigate. Until today, intermediate roads have been built in order to make excavation works easier and to connect the existing roads to each other in the ancient city of Teos (Fig. 3.6, Fig. 3.7 & Fig. 3.8). There has been an increase in the total road length to meet the need, especially with the increase in the urban population in the region (Table 5.1).

Table 5.1. Increment of  total road length over years

| Road Network (km) | Year | Change (%) |
|---|---|---|
| 23.13 | 1957 | 180 |
| 41.63 | 1986 | 190 |
| 79.10 | 2020 | - |

- For the soil erosion risk analysis, slope analyzes of the ruins in Teos were made and it was understood that the ruins with the highest soil erosion risk were Acropolis Theatre and partly Dionysos Temple (Table 4.4 & Table 4.5.).

- As a result of the watershed risk analysis, the ruins in the direction of the basin flow that may be under the influence of possible damage were observed as Acropolis, Theater and Bouleuterion (Table 4.6.).

- According to the selected hypothetical sea level rises, there would be no ruins to be affected at 1 meter of rise, while 3.8 meters and 5 meters of sea level rise would affect the vicinity of Bouleuterion.

- Based on the InSAR deformation results (Table 4.8), no significant data were obtained that could be evaluated. In future studies, a more detailed earthquake analysis should be done with higher resolution satellite images.

- As a result of the UAV images obtained by UAV flights (Fig. 3.28, Fig. 3.29, Fig. 3.30, Fig. 3.31 & Fig. 3.32) and the map created with these images (Fig. 3.27), the most up-to-date images of the ruins in Teos were obtained in high resolution. According to the images, it was observed that vegetation surrounds the Acropolis, Theater and Dionysus Temple. Southern Port, on the other hand, is notable for its obvious proximity to residences and restaurants used by people. The illegal construction around Teos was not reflected in the orthophoto images, but this situation was revealed in in-situ observations.

- Better results in PSI can be obtained with studies to be carried out by taking more detailed radar images.

- As a result of the Analytic Hierarchy Process, the most important risk factors threatening Teos were observed as Urban Sprawl, Proximity to Transportation Routes and Earthquake.

# CHAPTER 6
# CONCLUSION

This research aimed to reveal the current situation of Teos Ancient City against natural and human-induced risk factors. Based on the Analytical Hierarchy Process, in which all risk factors were considered together, it has been concluded that the most important risk factors were urban sprawl, proximity to transportation routes, earthquake, watershed, soil erosion, structural damage and coastal flood, in order of importance.

While analyzing the risk factors threatening Teos, it was understood that the most important and current risk factor was the urban sprawl, and the risk of proximity to transportation routes emerged as a result of urban sprawl.

Risk factors other than urban sprawl and proximity to transportation routes are nature-based risk factors, and if precautions are not taken, the impact area of natural risk factors will increase directly proportional with the increase in urban sprawl, and the affected area will not be limited to Teos, but the people in the irregular settlements around Teos will also be affected.

While examining factors such as urban sprawl (supervised classification), proximity to transportation routes and earthquake risk assessment, satellite images taken from different dates were used in the methodology in order to make comparisons and obtain detailed analysis data.

Each of urban sprawl and structural damage assessments were made using 2 different analyzes in order to address the time-dependent variation of both risk factors. It was sufficient to use a single method in the evaluation of other risk factors.

When the most recent high-resolution orthophoto images obtained were examined, it was observed that illegal construction and irregular vegetation cover the ruins of Teos. Based on these conclusions, irregular vegetation and illegal construction in the archaeological site should be checked in detail with both in-situ studies and regular UAV flights and necessary precautions should be taken.

Slope map of Teos Ancient City (Fig. 3.9) shows that the most hazardous ruins that can be affected because of soil erosion are Acropolis, Theatre and partly Dionysos Temple. Planting grass, adding mulch or rocks and using mulch matting to hold vegetation on slopes can be the solution to prevent soil erosion around the most at risk ruins of Teos.

Measures to shield ruins from exposure to exterior city, as well as probable excessive light exposure and high and changing temperature and humidity, could lessen the risk of possible damage to ruins.

In conclusion, this research is not limited to an initiative for the protection of Teos, which is a cultural asset, but also aims to comprehensively reveal the risk factors of cultural heritages both in Turkey and in various parts of the world using GIS and remote sensing, and to analyze these risk factors by using the Analytic Hierarchy Process.

## REFERENCES


Agapiou, A., Lysandrou, V., Alexakis, D. D., Themistocleous, K., Cuca, B., Argyriou, A., ... & Hadjimitsis, D. G. (2015). Cultural heritage management and monitoring using remote sensing data and GIS: The case study of Paphos area, Cyprus. *Computers, Environment and Urban Systems*, *54*, 230-239. https://doi.org/10.1016/j.compenvurbsys.2015.09.003

Bakak, Ö., Özel, E., & Ergün, M. (2015). Geothermal potential of the Sığacık Gulf (Seferihisar) and preliminary investigations with seismic and magnetic surveys. *Energy Procedia*, *76*, 230-239. https://doi.org/10.1016/j.egypro.2015.07.909

Centre for Research on the Epidemiology of Disasters United Nations Office for Disaster Risk Reduction, & Wallemacq, House, P. R. (2021, May 14). *Economic losses, poverty & disasters: 1998–2017*. UNDRR. https://www.undrr.org/publication/economic-losses-poverty-disasters-1998-2017

Chen, S. E., Liu, W., Bian, H., & Smith, B. (2013). 3D LiDAR scans for bridge damage evaluations. In Forensic Engineering 2012: Gateway to a Safer Tomorrow (pp. 487-495). https://doi.org/10.1061/9780784412640.052

Climate-data.org. (2022, April 14). *Climate graph and rain measures of Seferihisar*. Climate-data.org. https://en.climate-data.org/asia/turkey/izmir/seferihisar-21649/#climate-graph

Congedo, L., & Macchi, S. (2015). The demographic dimension of climate change vulnerability: exploring the relation between population growth and urban sprawl in Dar es Salaam. *Current Opinion in Environmental Sustainability*, *13*, 1-10.

D’Aranno, P. J., Di Benedetto, A., Fiani, M., Marsella, M., Moriero, I., & Palenzuela Baena, J. A. (2021). An application of persistent scatterer interferometry (psi) technique for infrastructure monitoring. *Remote Sensing*, *13*(6), 1052. https://doi.org/10.3390/rs13061052

Deelstra, T., & Girardet, H. (2000). Urban agriculture and sustainable cities. *Bakker N., Dubbeling M., Gündel S., Sabel-Koshella U., de Zeeuw H. Growing cities, growing food. Urban agriculture on the policy agenda. Feldafing, Germany: Zentralstelle für Ernährung und Landwirtschaft (ZEL)*, 43-66.

DeJarnett, N., Yeager, R., Conklin, D. J., Lee, J., O’Toole, T. E., McCracken, J., ... & Bhatnagar, A. (2015). Residential proximity to major roadways is associated with increased levels of AC133+ circulating angiogenic cells. *Arteriosclerosis, thrombosis, and vascular biology*, *35*(11), 2468-2477.

Diwedar, A. I. (2016). Investigating the effect of wave parameters on wave runup. *Alexandria Engineering Journal*, *55*(1), 627-633.

ESA. (n.d.-a). (May 6, 2022). *Sentinel-1 SAR Resolutions*. European Space Agency. https://sentinels.copernicus.eu/web/sentinel/user-guides/sentinel-1-sar/resolutions

ESA. (n.d.-b). (May 6, 2022). *SPOT 6*. European Space Agency. https://earth.esa.int/eogateway/missions/spot-6

Foody, G. M. (2002). Status of land cover classification accuracy assessment. *Remote Sensing of Environment*, *80*(1), 185-201.

Geoscience Australia. (April 30, 2022). *Applying Geoscience to Australia's Most Important Challenges.* https://www.ga.gov.au/scientific-topics/positioning-navigation/geodesy/geodetic-techniques/interferometric-synthetic-aperture-radar

Goepel, K. D. (May 4, 2022.). *AHP Online System - AHP-OS*. BPMSG - Business Performance Management Singapore. https://bpmsg.com/ahp/

Goepel, K. D. (2017). Implementation of an online software tool for the analytic hierarchy process—Challenges and practical experiences. Implement. *Online Softw. Tool AHP Chall. Pract. Exp*, *10*, 1-20.

Goepel, K. D. (2018). Implementation of an Online Software Tool for the Analytic Hierarchy Process (AHP-OS). *International Journal of the Analytic Hierarchy Process*, *10*(3). https://doi.org/10.13033/ijahp.v10i3.590

Google Maps. (2021, 14 December) *Location of Teos Ancient City.* Google Maps. https://www.google.com/maps/d/embed?mid=1AD1EltE6JYGM-RhYx9A7caSoalE&hl=en&ehbc=2E312F

Halicioglu, K., & Ozener, H. (2008). Geodetic network design and optimization on the active Tuzla fault (Izmir, Turkey) for disaster management. *Sensors*, *8*(8), 4742-4757.

Hooke, R. L., Martín Duque, J. F., & Pedraza Gilsanz, J. D. (2013). Land transformation by humans: a review. GSA Today.

Ilies, D. C., Caciora, T., Herman, G. V., Ilies, A., Ropa, M., & Baias, S. (2020). *Geohazards affecting cultural heritage monuments. A complex case study from Romania.* Research Square. https://www.researchsquare.com/article/rs-31190/v1

Jo, H. C., Sohn, H. G., & Lim, Y. M. (2020). A lidar point cloud data-based method for evaluating strain on a curved steel plate subjected to lateral pressure. *Sensors*, *20*(3), 721. https://doi.org/10.3390/s20030721

Kadıoğlu. (2012). Teos Guide Book [Brochure]. http://www.teosarkeoloji.com/multimedia/Teos_Rehber_Guide.pdf

Kadıoğlu. (2018). Teos Guide Book II [Brochure]. http://www.teosarkeoloji.com/documents/teos-guide-book-ii.pdf

Killeen, P. G., Mwenifumbo, C. J., & Ford, K. L. (2015). Tools and Techniques: Radiometric Methods. Treatise on Geophysics, 447–524. doi:10.1016/b978-0-444-53802-4.00209-8

Marfai, M. A., & King, L. (2008). Coastal flood management in Semarang, Indonesia. *Environmental geology*, *55*(7), 1507-1518.

Ngadiman, N., Kaamin, M., Sahat, S., Mokhtar, M., Ahmad, N. F. A., Kadir, A. A., & Razali, S. N. M. (2018, September). Production of orthophoto map using UAV photogrammetry: A case study in UTHM Pagoh campus. In *AIP Conference Proceedings* (Vol. 2016, No. 1, p. 020112). AIP Publishing LLC.

Olsen, M. J., Kuester, F., Chang, B. J., & Hutchinson, T. C. (2010). Terrestrial laser scanning-based structural damage assessment. *Journal of Computing in Civil Engineering*, *24*(3), 264-272. https://doi.org/10.1061/(ASCE)CP.1943-5487.0000028

Onat, O., Yön, B., Öncü, M. E., Varolgüneş, S., Karaşin, A., & Cemalgil, S. (2022). Field reconnaissance and structural assessment of the October 30, 2020, Samos, Aegean Sea earthquake: an example of severe damage due to the basin effect. *Natural Hazards*, 1-43. https://doi.org/10.1007/s11069-021-05173-y

Özacar, A. A., Gülerce, Z., Sopacı, E., & Askan Gündoğan, A. (2020). The October 30, 2020 İzmir-Seferihisar Offshore (Samos) Earthquake (Mw= 6.6) Reconnaissance Observations and Findings (Report No: METU/EERC 2020-03), 2: *Observations on İzmir Seferihisar Offshore (Samos) Earthquake and Active Tectonism*.

Polat, Y. (2016). *Teos hellenistik dönem savunma sistemi (Hellenistic defence system in Teos).* [Unpublished doctoral dissertation]. Gazi University.

Saha, A., & Roy, R. (2021). An integrated approach to identify suitable areas for built-up development using GIS-based multi-criteria analysis and AHP in Siliguri planning area, India. *SN Applied Sciences*, *3*(4), 1-17. https://doi.org/10.1007/s42452-021-04354-5

Samanta, S., & Koloa, C. (2014). Modelling coastal flood hazard using ArcGIS spatial analysis tools and satellite image. *Int. J. Sci. Res*, *3*, 961-967.

Scotland’s soils. (2021, May 18). *Map of soil erosion risk (partial cover)*. https://soils.environment.gov.scot/maps/risk-maps/map-of-soil-erosion-risk-partial-cover

*Sesli Sözlük*. (n.d.). Sesli Sözlük. Retrieved April 14, 2022, from https://www.seslisozluk.net/watershed-nedir-ne-demek

Sığacık. (2021, November 3). In *Wikipedia*. https://en.wikipedia.org/wiki/Sığacık

Siswanto, S. Y., & Sule, M. I. S. (2019, December). The Impact of slope steepness and land use type on soil properties in Cirandu Sub-Sub Catchment, Citarum Watershed. In *IOP Conference Series: Earth and Environmental Science* (Vol. 393, No. 1, p. 012059). IOP Publishing.

Sivakumar, M. V. (2005). Impacts of natural disasters in agriculture, rangeland and forestry: an overview. *Natural disasters and extreme events in Agriculture*, 1-22. https://doi.org/10.1007/3-540-28307-2_1

Teos. (2022, April 27). In *Wikipedia*. https://en.wikipedia.org/wiki/Teos

Türkiye İstatistik Kurumu (TÜİK). (2021, February 5). *Adrese Dayalı Nüfus Kayıt Sistemi Sonuçları, 2020*. TÜİK. https://data.tuik.gov.tr/Bulten/Index?p=Adrese-Dayali-Nufus-Kayit-Sistemi-Sonuclari-2020-37210

United States Environmental Protection Agency. (2014, August 16). *Near Roadway Air Pollution and Health: Frequently Asked Questions.* https://www.epa.gov/sites/default/files/2015-11/documents/420f14044_0.pdf

United States Environmental Protection Agency. (2022, April 29). *Watershed Academy Web: Watershed Ecological Risk Assessment*. U.S. Environmental Protection Agency. https://cfpub.epa.gov/watertrain/moduleFrame.cfm?parent_object_id=6

USGS. (2019, November 13). *How much water is there on earth? completed*. How Much Water is There on Earth? | U.S. Geological Survey. Retrieved August 7, 2022, from https://www.usgs.gov/special-topics/water-science-school/science/how-much-water-there-earth

*Urban sprawl.* (2021, July 24). Everything Connects. https://www.everythingconnects.org/urban-sprawl.html

Varotsos, C., Tzanis, C., & Cracknell, A. (2009). The enhanced deterioration of the cultural heritage monuments due to air pollution. *Environmental Science and Pollution Research*, *16*(5), 590-592.

Yakut, A., Sucuoğlu, H., Binici, B., Canbay, E., Donmez, C., İlki, A., ... & Ay, B. Ö. (2021). Performance of structures in İzmir after the Samos island earthquake. *Bulletin of Earthquake Engineering*, 1-26.